

DEPOSITIONAL ENVIRONMENTS AND DIAGENESIS OF
THE ATKINS SANDSTONE, PENNSYLVANIAN
TO PERMIAN, NORTHEASTERN
MIDLAND BASIN

By

GREGORY R. SIMMONS

Bachelor of Science

Oklahoma State University

Stillwater, Oklahoma

1978

Submitted to the Faculty of the Graduate College
of Oklahoma State University
in partial fulfillment of the requirements
for the Degree of
MASTER OF SCIENCE
July, 1982

Thesis
1982
S592d
Cop.3



DEPOSITIONAL ENVIRONMENTS AND DIAGENESIS OF
THE ATKINS SANDSTONE, PENNSYLVANIAN
TO PERMIAN, NORTHEASTERN
MIDLAND BASIN

Thesis Approved:

Cary F. Gensert

Thesis Adviser

Dr. Stanton M. Ball

John W. Shelton

Zuhair al-Sharck

Norman N. Durbin

Dean of the Graduate College

PREFACE

This thesis concerns the depositional environment and diagenesis of the Atkins Sandstone. The writer wishes to acknowledge his indebtedness to those involved from its inception to completion.

The utmost appreciation is extended to Amoco for providing the thesis problem, financial support, and various resources used for the research including base maps, company reports, cores and core photographs. Gratitude is extended to all of the Amoco staff involved, but especially to George Simmons for his support in persuading Amoco to sponsor this study, Dr. Mike R. Short for his advice and the use of his Atkins interval isopach map, Dr. Stanton M. Ball for his advice and dedicated service as a thesis committee member, and Jim Hardin for his help in acquiring the resources necessary for the research.

Equal regards are held for the other members of the thesis committee. The writer is grateful to Dr. Gary F. Stewart, committee chairman, and Dr. John W. Shelton for their guidance and careful review of the manuscript and plates. The writer wishes to acknowledge Dr. Zuhair Al-Shaieb for his guidance concerning diagenesis.

The writer wishes to thank Jeanne Vale and Mary Crain for their services as typists. The writer is deeply indebted to his parents for their love, support and encouragement. And finally, the writer wishes to acknowledge the support and encouragement of all of his friends, without whom this effort would carry little significance.

TABLE OF CONTENTS

Chapter	Page
I. ABSTRACT.	1
II. INTRODUCTION.	2
Objectives and Methods	2
Previous Investigations.	5
III. GEOLOGIC HISTORY.	8
IV. STRUCTURAL FRAMEWORK.	11
V. STRATIGRAPHIC FRAMEWORK	12
Correlation.	12
VI. GEOMETRY OF THE ATKINS SANDSTONE.	15
Atkins "A" Sandstone	15
Relative Location	15
Trend and Width	15
Thickness	15
Boundaries.	16
Atkins "B" Sandstone	16
Relative Location	16
Trend and Width	17
Thickness	17
Boundaries.	17
Atkins "C" Sandstone	17
Relative Location	17
Trend and Width	18
Thickness	18
Boundaries.	18
VII. INTERNAL FEATURES	19
Sedimentary Structures	19
Interstratification	23
Soft-sediment Deformation	23
Medium-scale Crossbedding	23
Ripple-Marks.	23
Massive Bedding	24
Bioturbation and Burrowing.	24
Nodules	24

Chapter	Page
Texture	24
Constituents	35
VIII. DEPOSITIONAL ENVIRONMENT	37
XI. DIAGENESIS OF THE ATKINS SANDSTONE	45
X. PORE GEOMETRY	56
XI. APPLICATIONS OF INVESTIGATION	58
XII. SUMMARY	60
SELECTED REFERENCES	62
APPENDIX - CRITERIA FOR DETERMINING SANDSTONE BED BOUNDARIES ON ELECTRIC LOGS	65

LIST OF FIGURES

Figure	Page
1. Map of Study Area With Respect to Major Geologic Features of the Region	3
2. Map of Study Area Including Geologic and Geographic Features, Oil Fields Producing From the Atkins Sandstone, and Type Locality of the Atkins Sandstone	4
3. Principal Late Pennsylvanian and Early Permian Stratigraphic Units on the Eastern Shelf of the Midland Basin, South of the Study Area.	7
4. Core Analysis and Description of the Honolulu Oil R. G. Maben No. 2, Sec. 2, Blk. B, J. Rodman Survey	20
5. Core Analysis and Description of the Honolulu Oil Newman Bros. No. 2, Sec. 2, J. B. Ward Survey.	21
6. Core Analysis and Description of the Honolulu Oil Stewart No. 1, Sec. 4, Blk. B, J. Rodman Survey	22
7. Interstratified Sandstone and Shale, Honolulu Oil Maben No. 2	25
8. Interstratified Sandstone and Shale, Honolulu Oil Newman Bros. No. 2	26
9. Scattered Intraformational Clasts, Wavy Shale Laminae, and Siderite Nodule, Honolulu Oil Maben No. 2	27
10. Sandstone Lending and Bioturbated Shale, Honolulu Oil Maben Oil No. 2	28
11. Soft Sediment Flowage, Honolulu Oil Newman Bros. No. 2. . .	29
12. Soft Sediment Flowage, Honolulu Oil Maben No. 2	30
13. Medium-scale Crossbedding, Honolulu Oil Maben No. 2	31
14. Medium-scale Crossbedding, Honolulu Oil Newman Bros. No. 2.	32
15. Massive Bedding, Honolulu Oil Maben No. 2	33
16. Burrowed to Mottled Appearance of Interstratified Sandstone and Shale, Honolulu Oil Maben No. 2	34

Figure	Page
17. Intraformational Conglomerate, Honolulu Maben No. 2	36
18. Schematic Diagram of the Study Area Prior to Atkins Sandstone Deposition, Portraying Depositional Topography.	38
19. Schematic Diagram of the Study Area Prior to Atkins Sandstone Deposition, Portraying Erosional Topography . .	39
20. Schematic Diagram of the Study Area Subsequent to Atkins "A" Sandstone Deposition, but Prior to Atkins "B" and "C" Sandstone Deposition.	42
21. Schematic Diagram of the Study Area Subsequent to Atkins "B" and "C" Sandstone Deposition.	44
22. Syntaxial Quartz Overgrowth Shown by Obvious Pre-Overgrowth Grain Boundary.	46
23. Glauconite Altered to Iron-Deficient Clay	47
24. Glauconite Pseudomatrix	48
25. (a) Ankerite Cement. Magnification 200X. (b) Energy Dispersive X-ray Analysis Displaying Iron Substitution. .	49
26. Partially Dissolved Feldspar Grain Forming Secondary Porosity.	51
27. (a) Partially Dissolved Feldspar Grain. Magnification 200X. (b) Energy Dispersive X-ray Analysis Displaying the Grain to be Potassium Feldspar.	52
28. Vermicular Kaolinite Filling Pore	53
29. Chlorite Lining Pore.	54
30. (a) Chlorite Lining Pore. Magnification 2000X. (b) Energy Dispersive X-ray Analysis Illustrating Almost Complete Iron Substitution	55

LIST OF PLATES

Plate

1. East-West Stratigraphic Cross Section A-A' and East-West Stratigraphic Cross-Section B-B'. In Pocket
2. North-South Stratigraphic Cross-Section C-C' and North-South Stratigraphic Cross-Section D-D'. In Pocket
3. Structural Contour Map of the Base of the "M" Zone. . . . In Pocket
4. Gross Interval Isopach Map. In Pocket
5. Net-Sandstone Isopach Map of the Atkins Interval. In Pocket

CHAPTER I

ABSTRACT

The Atkins Sandstone is thought to include delta-front and marine sands deposited on the slope of the northeastern Midland Basin. This interpretation is based primarily on stratigraphic relationships, sandstone geometry, and the geologic setting described through previous investigations.

Sand transported basinward of the Pennsylvanian to Permian shelf edge was deposited as bars along the northern edge of a mid-basin carbonate platform. Sand also was distributed over the carbonate platform in channels and as fans.

Composition of the Atkins Sandstone is suggestive of an igneous source area. The Wichita-Amarillo uplift is considered the major source. Contributions from the Ouachita uplift cannot be discounted.

Digenesis of the Atkins Sandstone occurred through several stages. The initial diagenetic trend was the reduction of primary intergranular porosity due to compaction and cementation. Subsequent dissolution of unstable constituents produced well developed secondary porosity. Precipitation of chlorite as grain coatings significantly increased the surface area adjacent to porosity by the development of micro-porosity, without significantly reducing total porosity.

CHAPTER II

INTRODUCTION

The area of investigation of the Atkins Sandstone encompasses over 800 square miles in the northeastern Midland Basin, within a stratigraphic interval directly overlying the Horseshoe Atoll (Adams and others, 1951) (Figure 1). Portions of Crosby, Dickens, Kent, and Garza Counties, Texas, make up the study area (Figure 2).

The Atkins Sandstone produces hydrocarbons in White River, Lyn-Kay, and SMS Fields (Figure 2); therefore, determination of sandstone genesis, distribution and diagenesis should provide information useful in exploration for similar hydrocarbon accumulations. Diagenetic products such as secondary porosity and authigenic precipitates can affect reservoir quality and preservation of that quality during drilling and production.

Objectives and Methods

The objectives of this investigation were to (1) interpret the depositional environment(s) of the Atkins Sandstone, (2) interpret the nature and sequence of diagenetic events that have affected the Atkins Sandstone, (3) to relate the depositional environments and diagenetic history so as to understand better and explore more efficiently the Atkins Sandstone and similar sandstone bodies.

The method used to determine depositional environment was to compare descriptions of the geologic setting, geometry, and internal

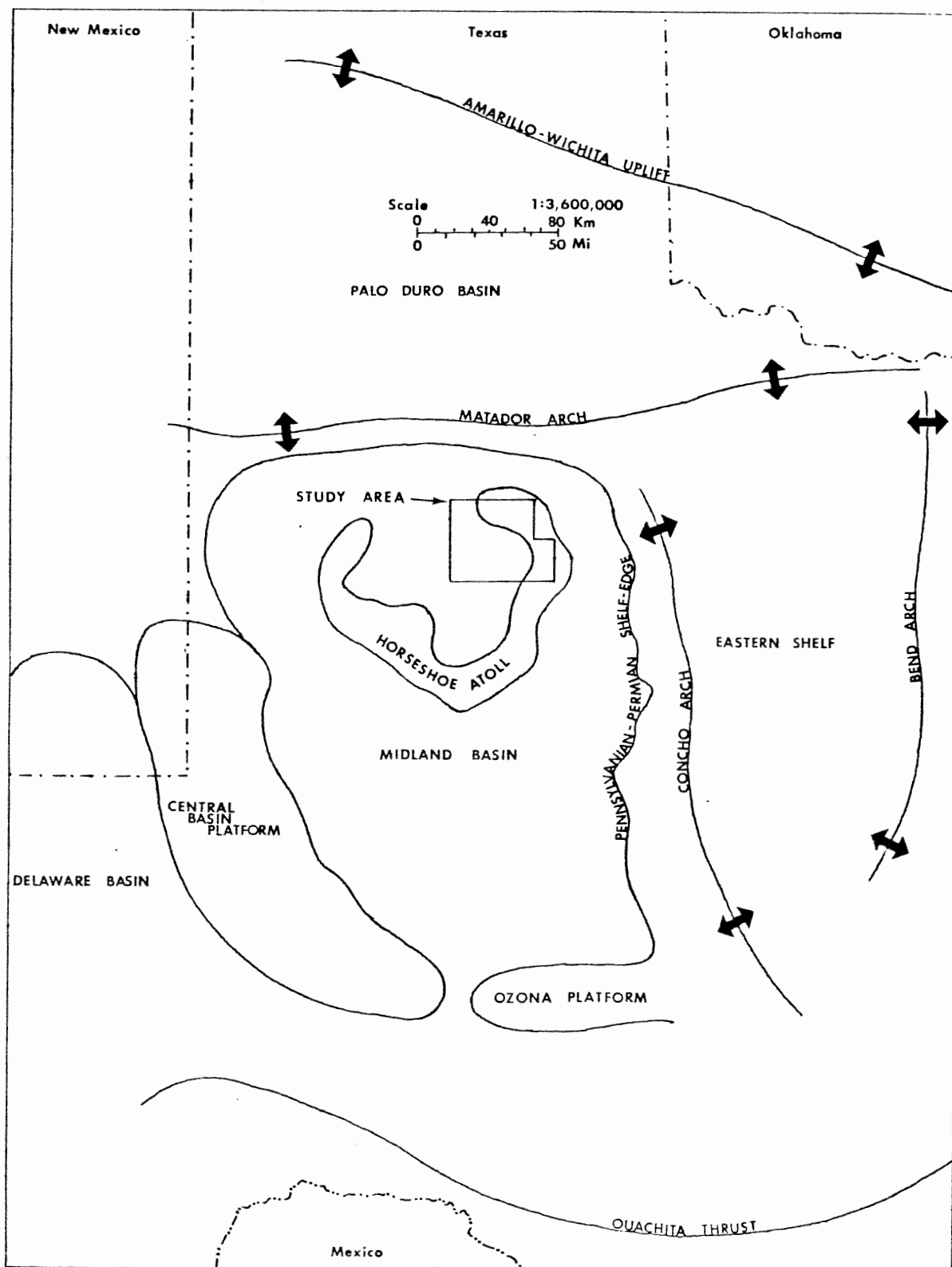


Figure 1. Map of Study Area With Respect to Major Geologic Features of the Region

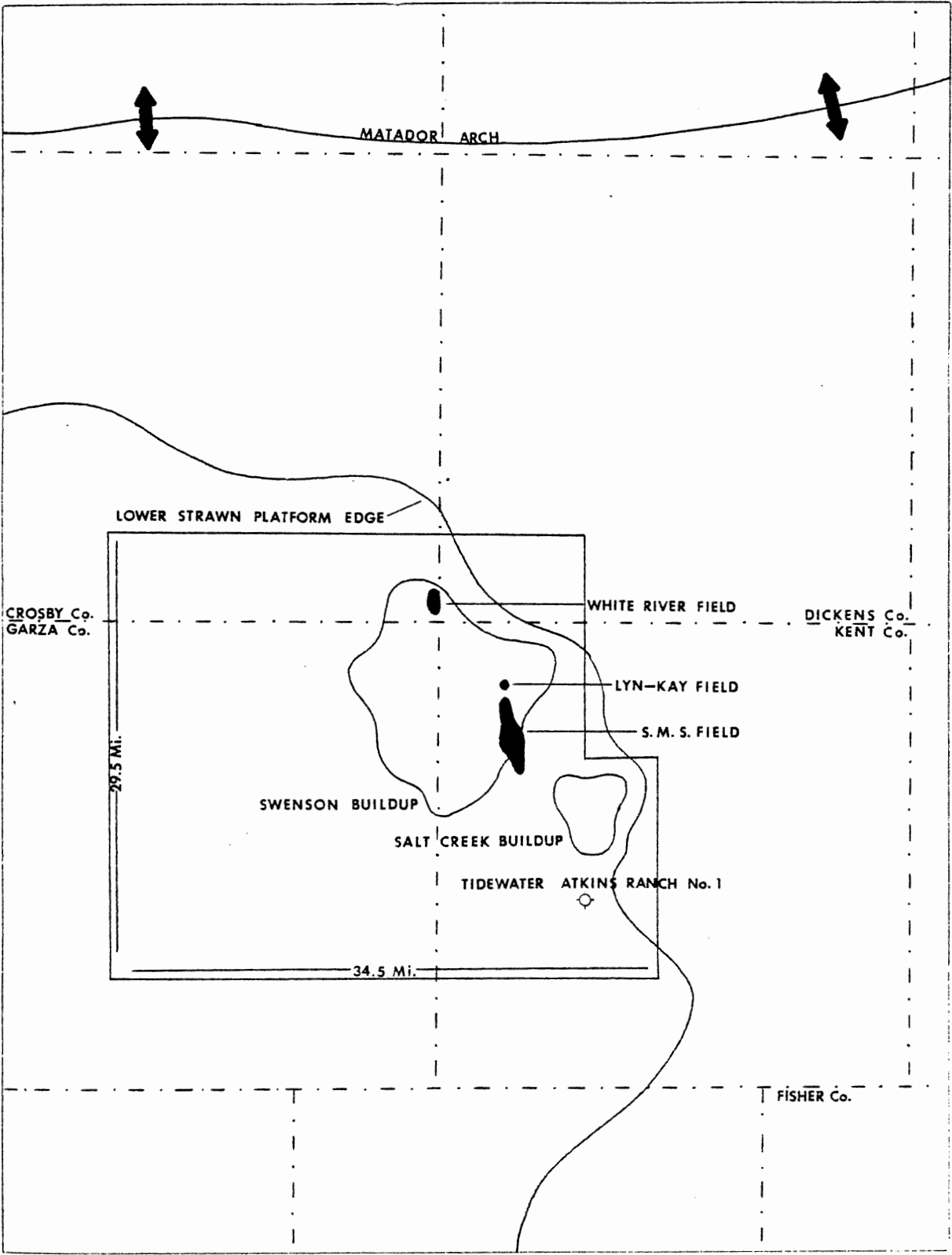


Figure 2. Map of Study Area Including Geologic and Geographic Features, Oil Fields Producing From the Atkins Sandstone, and Type Locality of the Atkins Sandstone

features of the Atkins Sandstone with those of documented depositional models (Shelton, 1973). Sandstone geometry (relative location, trend and width, thickness, and boundaries) were approximated by the preparation of four stratigraphic cross-sections, a structural contour map, a gross interval isopach map, and a net-sandstone isopach map (Plates 1 through 5). Internal features (sedimentary structures, textures, and constituents) were documented from the examination of three cores and forty thin sections. The diagenetic history was interpreted from the examination of the forty thin sections, corresponding X-ray diffractograms, and scanning-electron microscopy of selected representative samples.

Previous Investigations

The Pennsylvanian limestones of the underlying Horseshoe Atoll are highly productive petroleum reservoirs. Original reserves of the atoll were 2.5 billion barrels of oil (Wilson, 1975). Previous investigators and explorers largely ignored the overlying shale and sandstone due to the larger volume of reserves in the underlying limestones.

Earliest investigators of the atoll area considered the shales surrounding the atoll to be age-equivalent to the adjacent limestones. Sandstones interbedded within the surrounding shale were regionally termed the "Canyon Sands." However, Burnside (1959) stated that practically all of the surrounding shales are Wolfcampian. He based his reasoning on the observation that portions of the atoll crest are capped by Wolfcampian limestones, and that interstratification of limestone and shale was observed only near the crest of the atoll. Van Siclen (1958) was first to describe depositional topography on the eastern shelf and

slope of the Midland Basin. The Pennsylvanian to Permian shelf edge proposed by Van Siclen is consistent with that described later and in more detail by Bloomer(1977). According to Van Siclen's interpretation, the stratigraphic interval of interest in this study was deposited in a fondofom environment, age-equivalent to rocks overlying the Crystal Falls Limestone of the eastern shelf (Figure 3). Southeast of the study area, Bloomer (1977) investigated the Cook Sandstone (Figure 3). He traced the Cook Sandstone across the eastern shelf and slope of the Midland Basin and described fluvial, deltaic, and marine depositional systems. Several of Bloomer's findings are relevant to this study. The Pennsylvanian to Permian shelf edge was described as trending northward through Fisher County (Figure 1). If projected northward, this shelf edge would trend across extreme eastern Dickens County. Deltaic systems identified by Bloomer were proximal to the shelf edge. Upper delta-plain facies were deposited on the shelf. Thick sandstones basinward of the shelf edge were interpreted as distributary-mouth bars that graded basinward into prodelta facies. Bloomer described the eastern slope as having had a maximal regional dip of about 3° at midslope, which decreased basinward. Clastic wedges on the slope, basinward of the deltaic systems, were interpreted as marine channels and fans.

Baker (1975) noted the similarity in stratigraphic position of the Atkins Sandstone at SMS Field (Figure 2) and the Tannehill Sandstone (Figure 3) in Dickens County (Plate 1). Ball and Short (1979) explored an alternate explanation for the origin of Horseshoe Atoll. Previously interpreted "reef" masses may be erosional remnants standing above a nearly planar subaerial paleo-erosional surface.

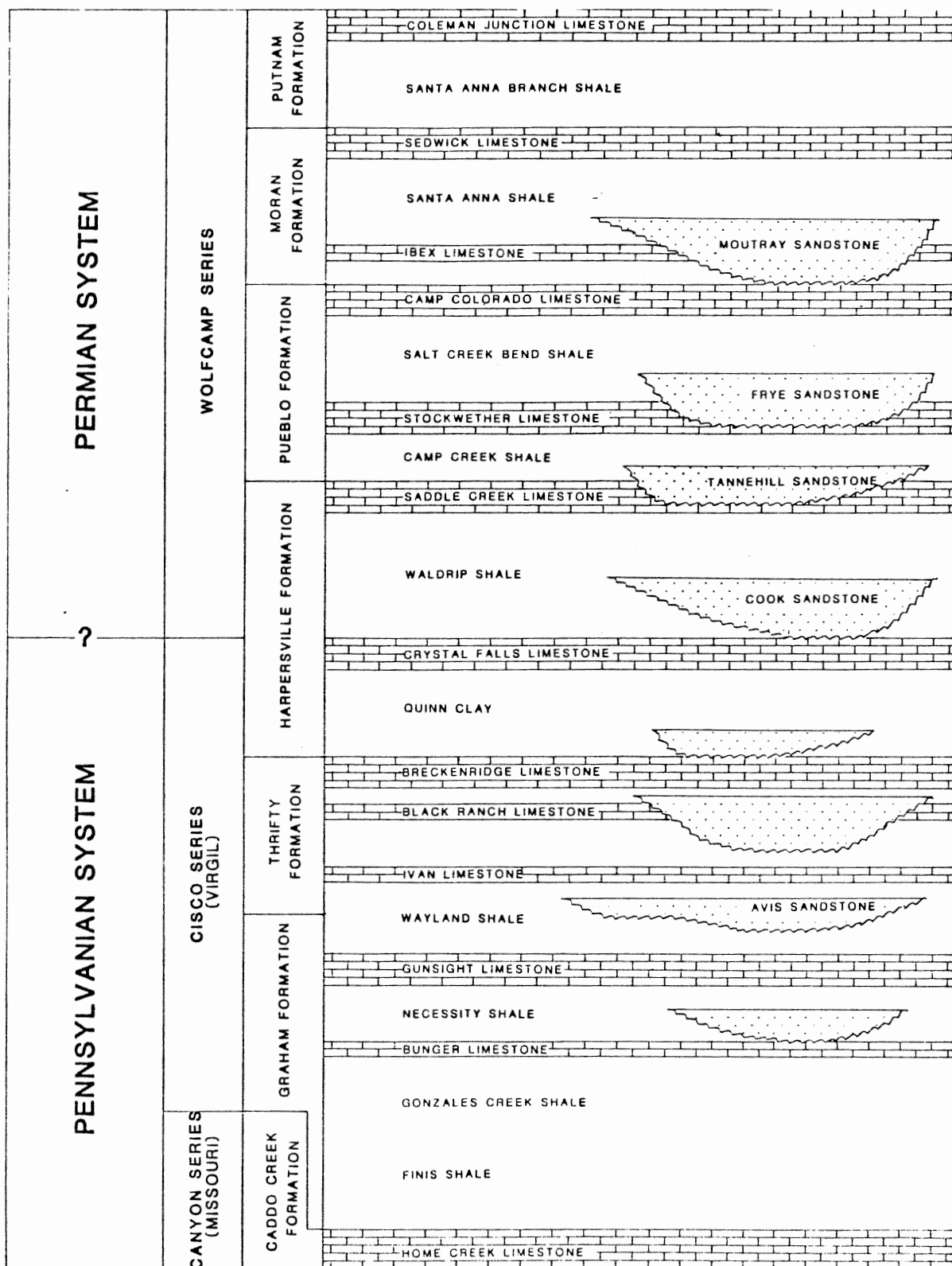


Figure 3. Principle Late Pennsylvanian and Early Permian Stratigraphic Units on the Eastern Shelf of the Midland Basin, Southwest of the Study Area. After Brown (1969) and Bloomer (1977)

CHAPTER III

GEOLOGIC HISTORY

The Permian Basin of West Texas and southeast New Mexico is a composite basin occupying approximately 115,000 square miles (Galley, 1955). It consists of several major centers of deposition including the Midland Basin (Sellards, 1934) where the study area is located (Figure 1). The Central Basin Platform (Cartwright, 1930) (Figure 1) separates the Midland Basin from the structurally deeper Delaware Basin (Willis, 1929) (Figure 1). The Ouachita folded belt (Figure 1) is the major southern limit of the Permian Basin complex, but the southern limit of the Midland Basin is defined by the Ozona Platform (Vertrees, 1953) (Figure 1). The Val Verde Basin (Lewis, 1941) (Figure 1) south of the Ozona Platform existed as a late Paleozoic center of deposition within one of several troughs present in front of the Ouachita folded belt. The eastern shelf of the Midland Basin is limited by the Bend Arch (Cheney, 1918) (Figure 1). The Concho Arch (Cheney, 1929) (Figure 1) is a low, broad anticline extending south-southeastward across the eastern shelf. Separating the Midland Basin from the Palo Duro Basin (Figure 1) is a narrow belt of anticlines known as the Matador Arch (Totten, 1954). The Palo Duro Basin is limited on the north by the Amarillo-Wichita Uplift (Gould and Lewis, 1926) (Figure 1).

Prior to Pennsylvanian sedimentation, deposition occurred during several marine invasions on a broad, shallow, southward-dipping shelf. The rocks consist of transgressive clastics grading into carbonates.

The first invasion began in Late Cambrian. Regression at the close of the Mississippian Period was accompanied by several uplifts which drastically altered previous controls on sedimentation across the area. Affecting the Midland Basin area were the Ouachita, Amarillo-Wichita, and Matador Uplifts. Thinning of Mississippian rocks provides evidence of local uplifts along the Central Basin Platform, and rejuvenation of the Concho Arch. (The paragraph above was drawn from the work of Galley, 1955.)

Pennsylvanian sedimentation occurred in an expanding sea within an intracratonic basin. Regional submergence began early in Strawn time and appears to have persisted at least periodically through the Permian Period, as shown by thick consecutive series of strata. Pennsylvanian sedimentary rocks along the basin margins include Strawn, Canyon, and Cisco beds. Large volumes of clastic sediments accumulated along basin margins adjacent to mountainous land masses, whereas in marginal areas more remote from clastic sources thick sections of limestone were deposited. Cyclic sequences are characteristic of the transitional areas between the carbonate and clastic depocenters. Terrestrial and deltaic deposits interbedded with marine sediments suggest shoreline fluctuation throughout the Late Pennsylvanian. Sediments of like ages with the middle of the basin consist of thin, dark, nonfossiliferous shales. Wells in the deep parts of the basin have penetrated thin sections of Upper Pennsylvanian strata. The term "starved basin" has been applied to describe the apparent lack of sedimentation within the middle part of the basin (Adams and others, 1951).

Horseshoe Atoll is different from the thin section of Upper Pennsylvanian rocks within the mid-basin area; according to some

geologists subsidence appears to have been matched by deposition of limestone. The atoll is interpreted as an arcuate accumulation of fossiliferous limestone apparently built upon a Lower Strawn platform; it is composed of limestones of the Strawn, Canyon, Cisco, and Wolfcamp Groups. The thickest section of the buildup exceeds 3000 ft. with age-equivalent basinal strata being thinner than 500 ft. (Wilson, 1975).

Determination of age relationships within the buildup is complex, because of reworked and mixed fusulinids of various ages. Apparently rocks of Cisco age are not present over the entire complex, and Wolfcampian rocks are very isolated. Rock within the buildups primarily are of detrital origin. Colonial organisms are very rare. Numerous shale breaks can be correlated for considerable distances within the buildups. The upper surface of the atoll consists of knolls and depressions, and the flanks slope gently away from the crest. (These facts suggest that relief of the atoll may not have been due to constructional processes.)

At the close of the Pennsylvanian Period the entire Central Basin Platform was uplifted. The Midland Basin was a separate intracratonic basin at this time (Galley, 1955). Related tectonic activity may have affected the northern Midland Basin at this time, as relief on the surface of Pennsylvanian limestone terrain may be due to extensive pre-Permian erosion.

Throughout the Permian Period marginal platforms were the sites of thick carbonate buildups. Adjacent low areas received chiefly fine-grained clastics. In the latter part of the Permian Period, the basin was the site of deposition under evaporitic conditions within a shrinking sea (Galley, 1955).

CHAPTER IV

STRUCTURAL FRAMEWORK

The regional structural configuration of the Pennsylvanian to Permian rocks across the study area is that of gentle westward dip, averaging approximately 50 ft. per mile (Plate 3). The Garza Arch is a very subtle fold that trends southeastward through Garza County; it is recognizable on structural contour maps of Lower Pennsylvanian strata. The Garza Arch is not obvious on the "M" zone structural contour map (Plate 3). Regional westward dip is interrupted locally by subtle noses and synclines. These subtle structures can be observed to occur above and adjacent to the limestone buildups of the atoll complex. They are interpreted as being the results of differential compaction within varying thicknesses of the Lower Black Shale. These subtle structures seem to have influenced entrapment in SMS and White River Fields where the Atkins Sandstone is the productive reservoir.

CHAPTER V

STRATIGRAPHIC FRAMEWORK

The Atkins Sandstone is present in the northeastern Midland Basin, adjacent to the Swenson and Salt Creek buildups, extending across southeastern Crosby, southwestern Dickens, western Kent, and eastern Garza Counties (Figure 2). The Atkins Ranch, type locality for the Atkins Sandstone, is in the southeastern part of the study area. Tidewater Oil Assoc. recovered oil and water on a drill-stem test of the Atkins Sandstone at the Atkins Ranch No. 1 before completing the well as a dry hole. The Atkins Sandstone is interbedded within the lower "Limestone Shale," overlying Pennsylvanian limestones and underlying the "M" zone, a widespread and easily recognizable marker bed that extends through the study area (Plates 1 and 2). On sample logs the "M" zone is described as glauconitic limestone. Thickness of the predominantly shale section between the Pennsylvanian limestones and the base of the "M" zone, herein to be referred to as the Atkins interval, ranges from 0 ft. in northwestern Kent County to about 950 ft. in central Kent County (Short, Amoco) (Plate 4). The exact age of the Atkins interval is unknown, but it is either in the Cisco or the Wolfcampian Series.

Correlation

Four stratigraphic cross-sections were prepared using the "M" zone as a datum (Plates 1 and 2). Correlations were made within the Atkins interval. Apparent stratigraphic relationships included topographic

relief on the top of the Pennsylvanian limestones (Plates 1 and 2), and the presence of sandstone and limestone at the stratigraphic position of the Atkins Sandstone in territory outside of the study area (Plate 1). Distribution and geometry of the Atkins Sandstone within the study area are also shown in general fashion by Plates 1 and 2.

The Atkins interval ranges from 0 to 950 ft. thick within the study area. Thinning of the interval is interpreted as reflecting topographic relief on top of the Pennsylvanian limestones. Two distinct limestone buildups are within the study area (Plate 4). The Swenson buildup (Figure 2) in northwestern Kent County was more than 600 ft. high, and it extended across about 150 sq. mi. In 3 to 4 sq. mi. of this area the relief of the buildup exceeded the stratigraphic position of the "M" zone (as implied by Plate 4, within the 100-ft. contour line). The crest of the Swenson buildup is capped by Cisco limestones (Vest, 1968, in Wilson, 1975, p. 188). The Salt Creek buildup (Figure 2) in northwestern to central Kent County occupies an area of approximately 15 square miles; it was approximately 450 ft. high. The crest of the Salt Creek buildup is 175 ft. below the stratigraphic position of the "M" zone, and is capped by Canyon limestone (Vest, 1968). These buildups overlie a Lower Strawn platform (Figure 2), the top of which is 650 ft. to 950 ft. below the base of the "M" zone. Deposition of the Atkins Sandstone and stratigraphically equivalent sandstone bodies was influenced by the topographic relief of the limestone surface.

The Atkins Sandstone occurs adjacent to and basinward of the Swenson and Salt Creek buildups. Tannehill Sandstone is present at the same stratigraphic position through most of Dickens and north-central to northeastern Kent Counties. Although not physically connected, the

Tannehill and Atkins Sandstones may be genetically related. The pinchout of the Tannehill Sandstone to the west of the northeastern edge of the Lower Strawn platform is shown on cross-section A-A' (Plate 1) between wells 9 and 10. The Tannehill Sandstone in Dickens County has been interpreted as widespread, massive, prograded distributary-mouth bars (Baker, 1975).

In southeast-central Crosby County the stratigraphic position of the Atkins Sandstone is occupied by several lenticular beds of limestone. The pinchout of the Atkins Sandstone and corresponding presence of these limestones is between wells 1 and 4 of cross-section A-A' (Plate 1). On sample logs the limestone is described as white to light tan to light gray, micritic to finely crystalline, oolitic, fossiliferous, and sandy.

The sandstone bodies considered to be Atkins Sandstone in this study are confined mostly to southeastern Crosby, extreme southwestern Dickens, western Kent, and eastern Garza Counties. Two major changes in geometry are suggestive of possibly three separate environments of deposition.

CHAPTER VI

GEOMETRY OF THE ATKINS SANDSTONE

Vertical division of the Atkins interval for the purpose of discussion is impractical because of the absence of suitable marker beds within the interval. Therefore, the interval will be discussed geographically with respect to major changes in sandstone geometry. These geographic divisions are designated as the Atkins "A", "B", and "C" Sandstones.

Atkins "A" Sandstone

Relative Location

The Atkins "A" Sandstone is present across southeastern Crosby, extreme northern Garza, and extreme southwestern Dickens Counties along the northern edge of the Lower Strawn platform (Plates 1 and 5).

Trend and Width

The Atkins "A" Sandstone extends north of the study area; thus the total extent is unknown. The relative trend appears to be east-northeast for a distance of approximately 30 mi. through the northern part of the study area (Plate 5).

Thickness

The Atkins "A" Sandstone is best developed in southeastern Crosby

County (Plates 1 and 5). Net-sandstone thickness ranges from 0 to 170 ft., whereas the total sandstone-interval is as thick as 300 ft.

The most commonly used method for determining sandstone-shale bed boundaries and thus net-sandstone thickness was to pick the inflection points of spontaneous-potential curve deflections. In cases where spontaneous-potential curve quality was inadequate, apparently from approximate equality in resistivity between formational fluids and drilling mud, a logical set of alternative methods were used to estimate net-sandstone thickness (Appendix).

Boundaries

Individual sandstone bodies of the Atkins "A" Sandstone are widespread. Generally they show gradational lower contacts (Plate 1). The lowest sandstone body is an exception; less extensive than the overlying sandstones, it has a sharp lower contact. Upper sandstone contacts are generally sharp. Lateral contacts invariably are interfingered.

Atkins "B" Sandstone

Relative Location

The Atkins "B" Sandstone is a linear belt in the northern part of the study area, extending along the Crosby-Dickens county line to northwestern Kent County. Along the Crosby-Dickens county line the Atkins "B" Sandstone produces at White River Field and across northwestern Kent County it produces at Lyn-Kay and SMS Fields (Figure 2). The Atkins "B" Sandstone overlies the Atkins "C" Sandstone to the south (Plates 2 and 5).

Trend and Width

The Atkins "B" Sandstone trends roughly northward (Plate 5). From the Crosby-Dickens county line it extends across northwestern Kent County above the eastern flank of the Swenson buildup. The length of this trend exceeds 15 mi. The distance that this trend might extend northward of White River Field, beyond the study area, was not determined. Width of the Atkins "B" Sandstone is approximately 1 to 2 mi. (Plates 1 and 5), increasing gradually to the south.

Thickness

The Atkins "B" Sandstone is best developed in northwestern Kent County where it is the productive reservoir at SMS Field. The maximal net-sandstone thickness is approximately 75 ft. (Plate 5).

Boundaries

The basal and lateral contacts of the Atkins "B" Sandstone are sharp. The upper contact ranges from gradational to moderately sharp (Plate 2).

Atkins "C" Sandstone

Relative Location

The Atkins "C" Sandstone is present across eastern Garza and west-central Kent Counties (Plates 2 and 5). Two distinct elongated sandstone lobes or clastic wedges occur adjacent to the Swenson buildup.

Trend and Width

The clastic wedge in Garza County roughly trends south-southwestward for a distance of approximately 30 mi., with a maximal width of approximately 15 mi. (Plate 5). The clastic wedge in Kent County trends roughly south-southeastward for approximately 15 mi., with a maximal width of approximately 8 mi.

Thickness

The Atkins "C" Sandstone is best developed over topographically low areas of the Lower Strawn platform (Plate 2). Net-sandstone thickness ranges from 0 to 270 ft. (Plate 7). Total sandstone-interval thickness is approximately 500 ft. The upper sandstone surface is relatively flat, and the increase in thickness is at the expense of the underlying shale.

Boundaries

The basal contact is sharp to the down-slope point of maximum sandstone thickness. Basinward of this point the lower contact is generally gradational (Plate 2). Lateral contacts adjacent to the limestone buildup are sharp, whereas the basinward lateral contacts are interfingered (Plates 1 and 2). Upper sandstone contacts generally are relatively sharp.

CHAPTER VII

INTERNAL FEATURES

Internal features were determined from a limited selection of cores. Three cores were selected for petrologic and petrographic study of the Atkins Sandstone, based on completeness and condition of the cores. All cores available were restricted to the Atkins "B" Sandstone from SMS Field.

Sedimentary Structures

In approximate order of overall abundance, sedimentary structures are interstratification of sandstone and shale with associated ripple-bedding (Reinecke and Wunderlich, 1968), small-scale crossbedding, soft-sediment loading and flowage, medium-scale crossbedding, ripple marks, massive bedding, bioturbation and burrowing, and nodular siderite (Figures 4, 5, and 6).

The sandstone beds invariably show sharp basal contacts which commonly are deformed by load structures. Beds of sandstone generally are overlain by interstratified sandstone and shale. Sharp and transitional contacts were observed between the sandstone and interstratified sandstone and shale. Thin beds of shale are relatively uncommon.

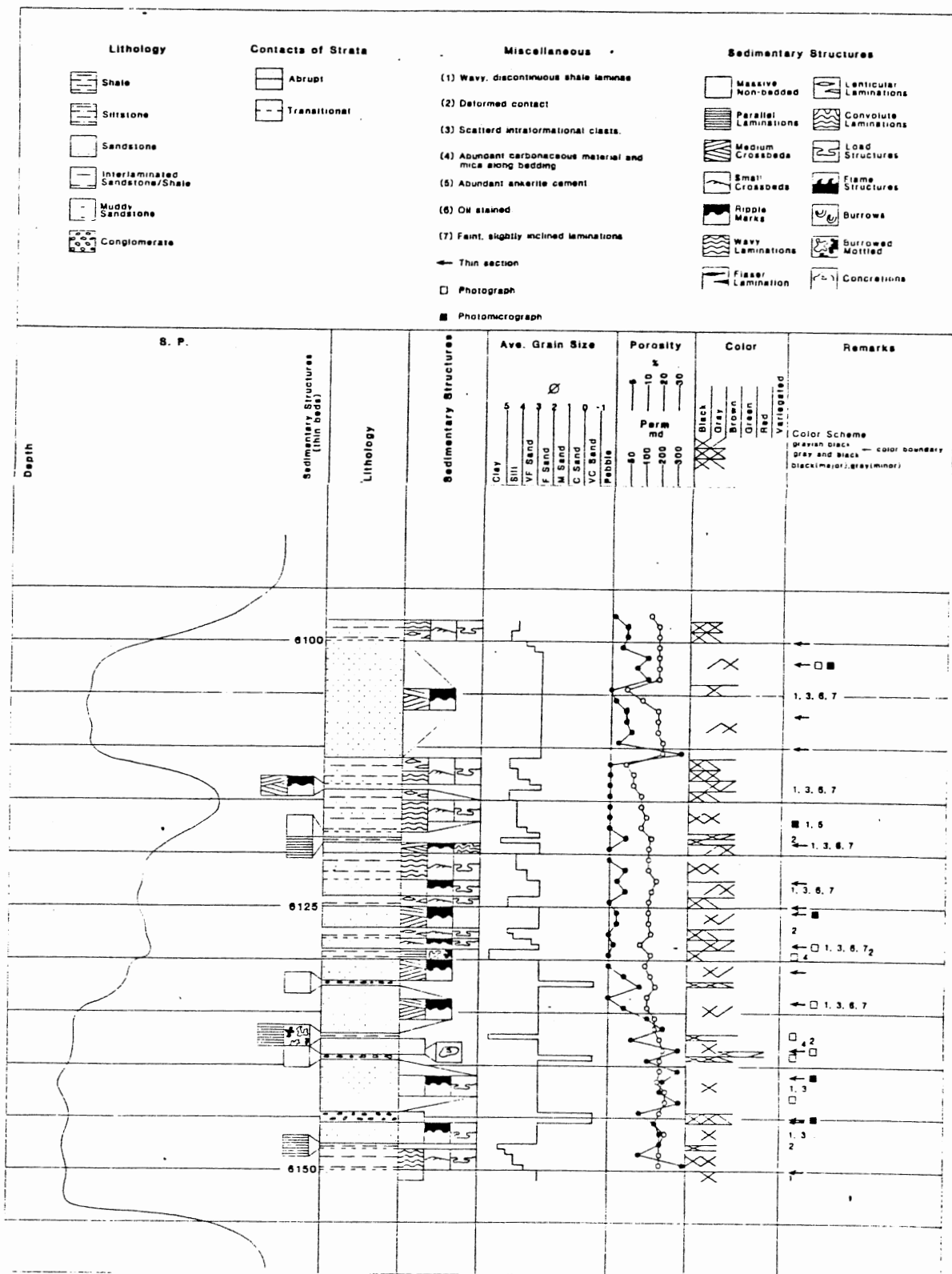


Figure 4. Core Analysis and Description of the Honolulu Oil R. G. Maben No. 2, Sec. 2, Blk. B, J. Rodman Survey

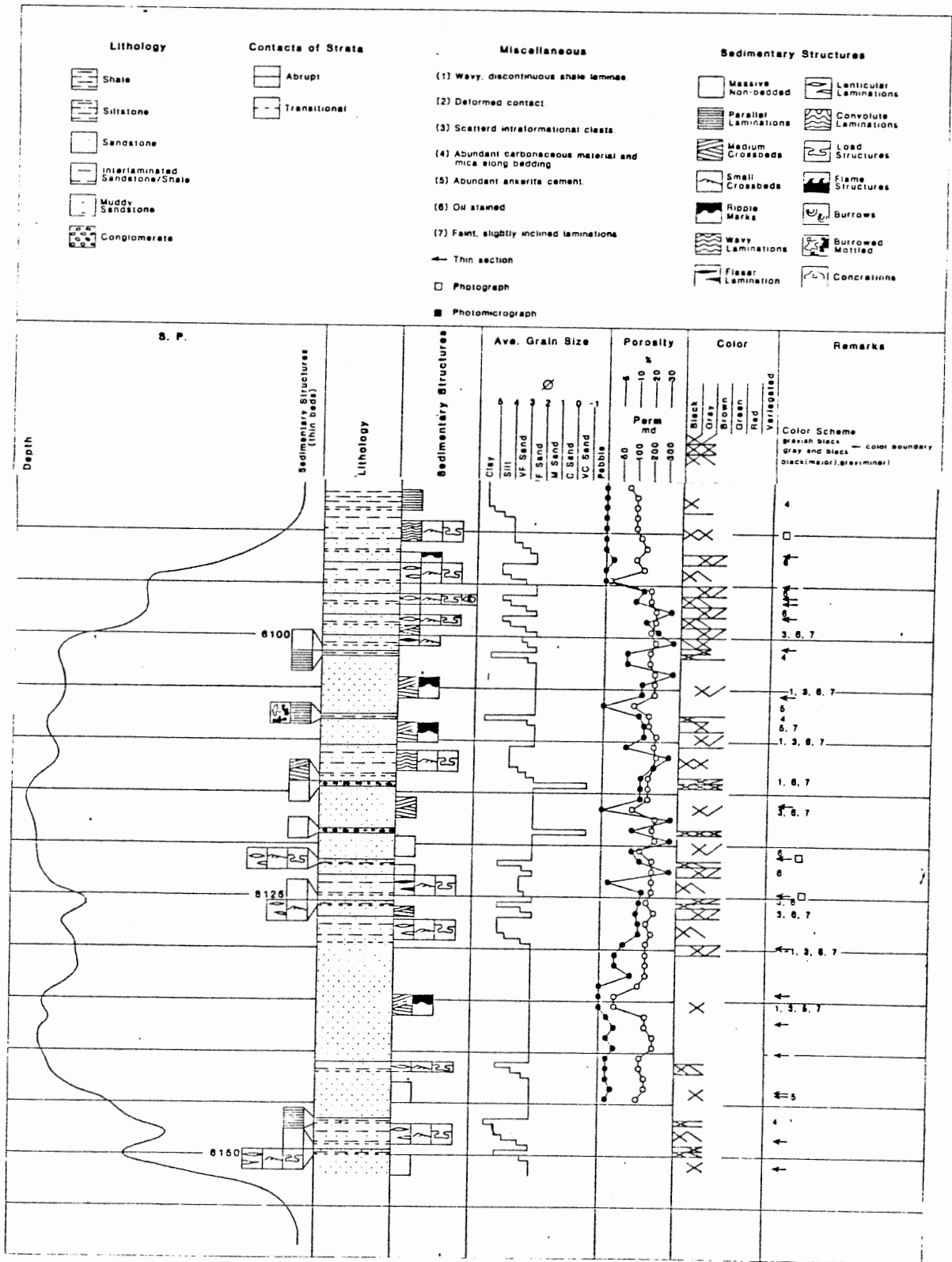


Figure 5. Core Analysis and Description of the Honolulu Oil Newman Bros. No. 2, Sec. 2, J. B. Ward Survey

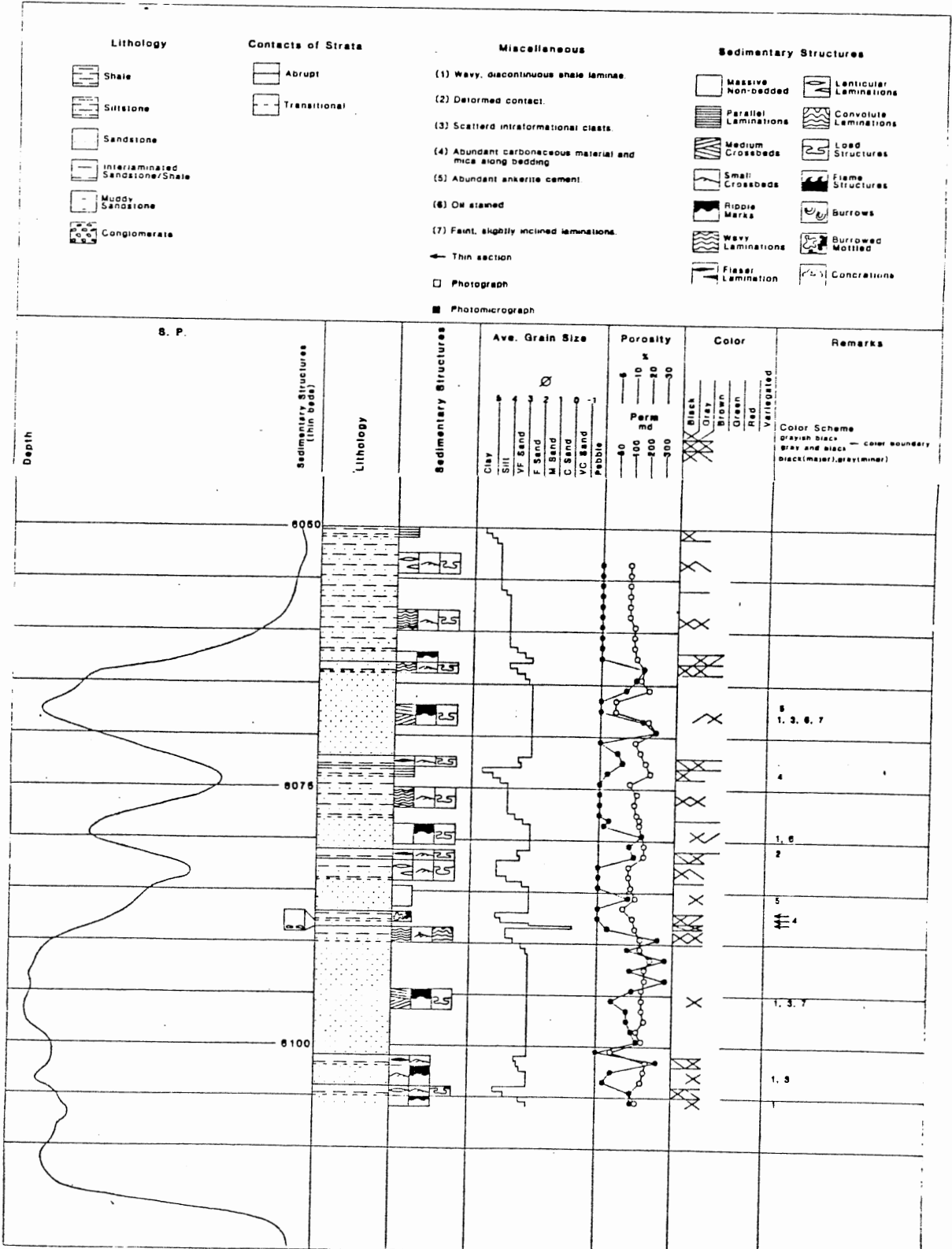


Figure 6. Core Analysis and Description of the Honolulu Oil Stewart No. 1, Sec. 4, Blk. B, J. Rodman Survey

Interstratification

Interstratification of sandstone and shale in the form of ripple-bedded units seems to be the most common sedimentary structure in the Atkins Sandstone. The complete range of ripple-bedding types is present, but wavy and lenticular bedding are the most abundant. Sandstone laminae contain small-scale crossbedding, whereas the intercalated shales are characterized by parallel laminations (Figures 7 and 8).

Sandstone beds are sparsely interstratified with thin shale laminae (Figure 9). These laminae are discontinuous and generally are characterized by a wavy appearance.

Soft-sediment Deformation

Soft-sediment deformation was observed to be most associated with the interstratified sandstone and shale section. Load structures (Figures 10 and 11) are most abundant, but flowage (Figure 12) is not uncommon.

Medium-scale Crossbedding

Medium-scale crossbedding is characteristic of thick sandstone beds and is recognizable as variably inclined, faint, parallel laminations and shale breaks (Figures 13 and 14). The laminations are more evident above the oil-water contact (Figure 15). Oil staining possibly enhances the visibility of the faint laminations.

Ripple Marks

The upper contacts of sandstone beds commonly are sharp, wavy.

undulating surfaces (Figure 7). These undulations are interpreted as ripple marks. The wavy shale laminae within the sandstone beds, discussed under interstratification, are assumed to have been draped over rippled sand surfaces (Figure 9).

Massive Bedding

Massive bedding is common to all cores within sandstone beds below the oil-water contacts (Figure 15). If oil staining has enhanced the visibility of the faint laminations, the massive appearing sandstone could possess a similar degree of bedding.

Bioturbation and Burrowing

Bioturbation and burrows are uncommon in the cores described. Several thin shale beds with abundant carbonaceous material had a mottled appearance (Figure 10). One interstratified section had a burrowed appearance (Figure 16).

Nodules

Nodules are rare in the Atkins Sandstone. Those present are sideritic (Figure 9). The nodules appeared to have been transported.

Texture

The Atkins Sandstone seems to be texturally mature; samples from cores show that sorting and rounding are good. Grain size ranges from very fine-grained sand to pebbles. Grain size is on the average of 0.125 mm. Significant vertical changes in grain size are not apparent within individual beds of sandstone. Intraformational clasts are the

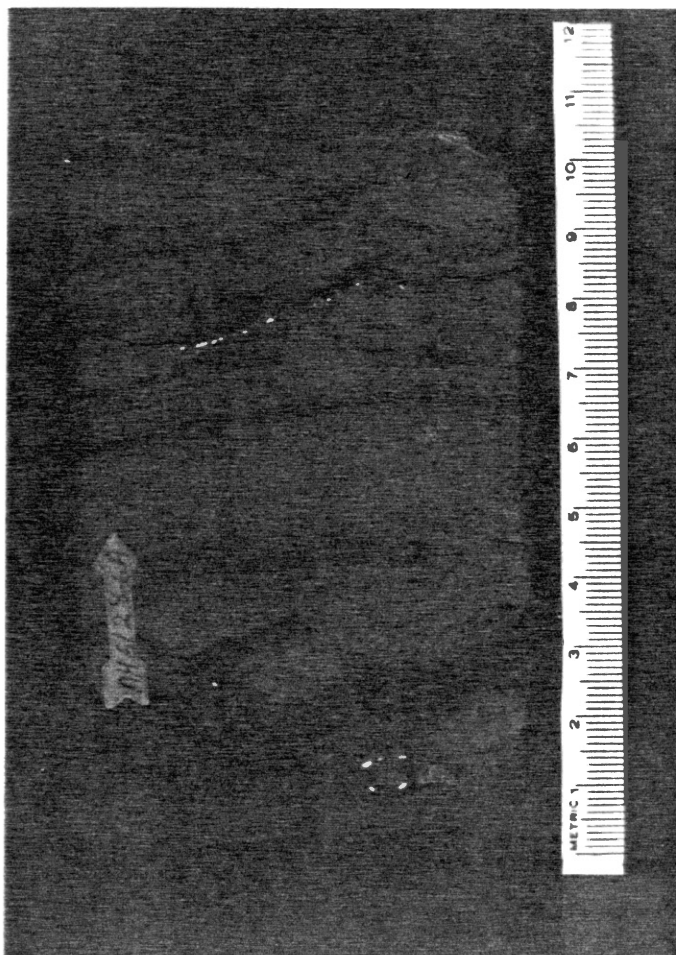


Figure 7. Interstratified Sandstone and Shale, Honolulu Oil Maben No. 2, Depth 6128.6 Ft. Note the Deformed Lower Sandstone Contacts, Rippled Upper Sandstone Contact, and Small-Scale Crossbedding. Depth Shown on Arrow.

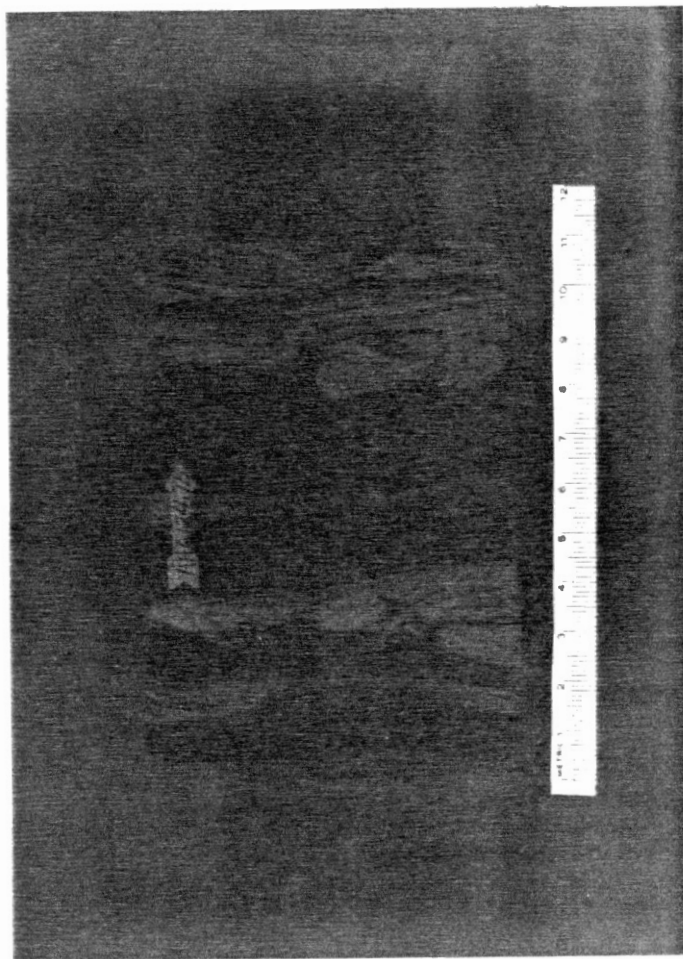


Figure 8. Interstratified Sandstone and Shale, Honolulu Oil Newman Bros. No. 2. Depth 6124.7 Ft. Shown on Arrow

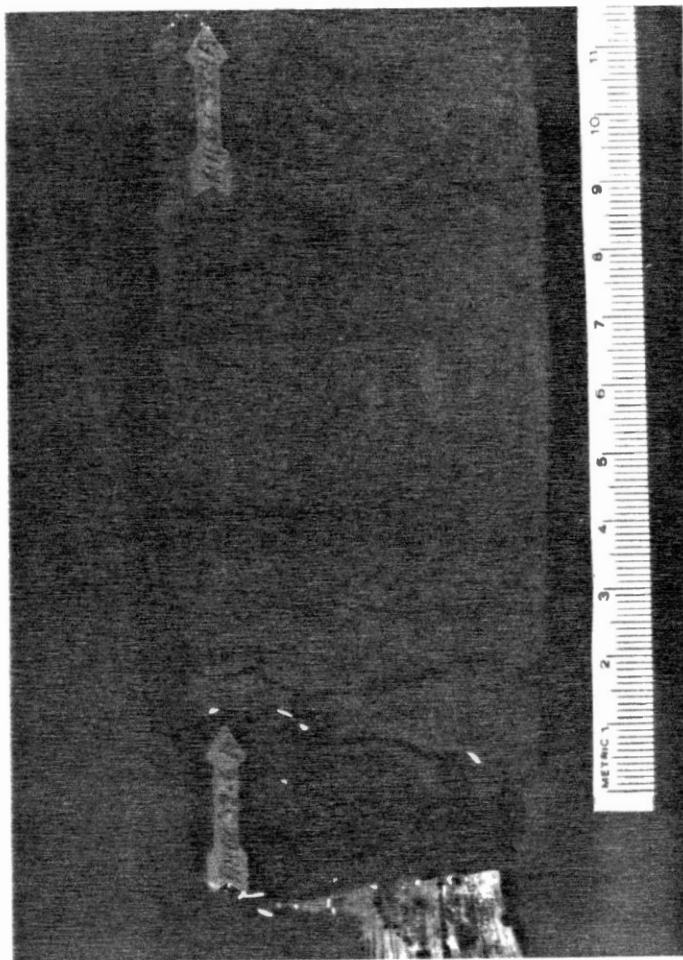


Figure 9. Scattered Intraformational Clasts, Wavy Shale Laminae, and Siderite Nodule, Honolulu Oil Maben No. 2. Depth 6138.6 Ft. Shown on Arrow

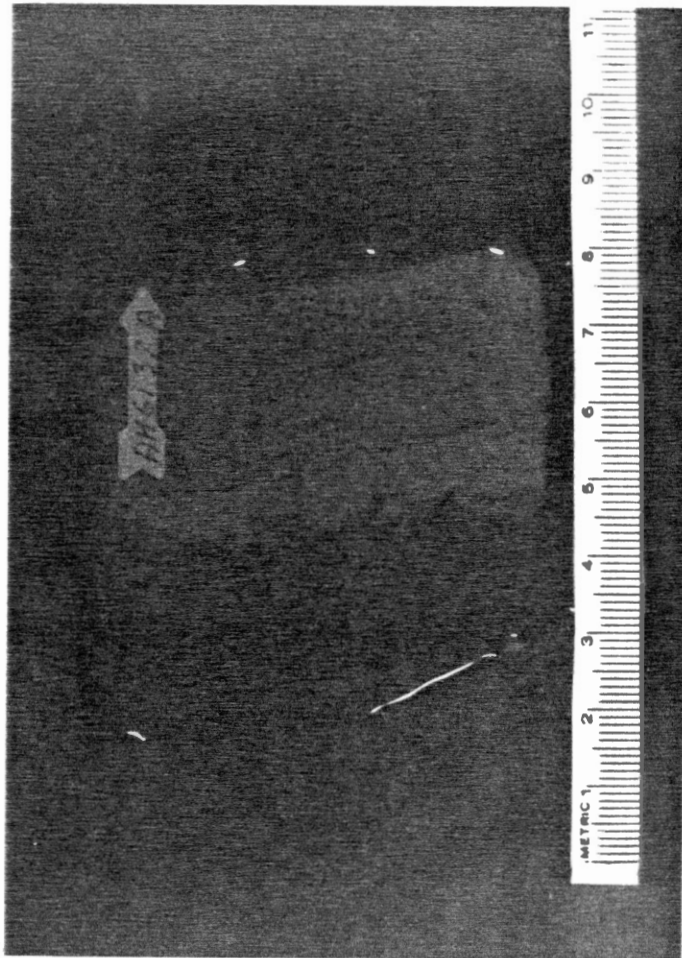


Figure 10. Sandstone Loading and Bio-turbated Shale, Honolulu Oil Maben No. 2. Depth 6137 Ft. Shown on Arrow

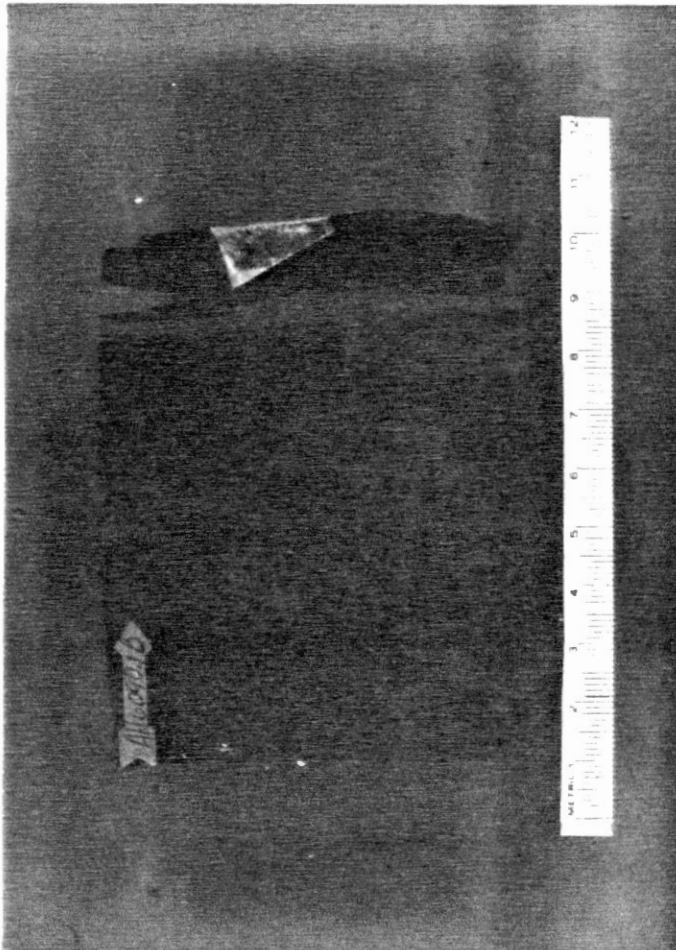


Figure 11. Soft Sediment Flowage,
Honolulu Oil Newman Bros.
No. 2. Depth 6090.1 Ft.
Shown on Arrow

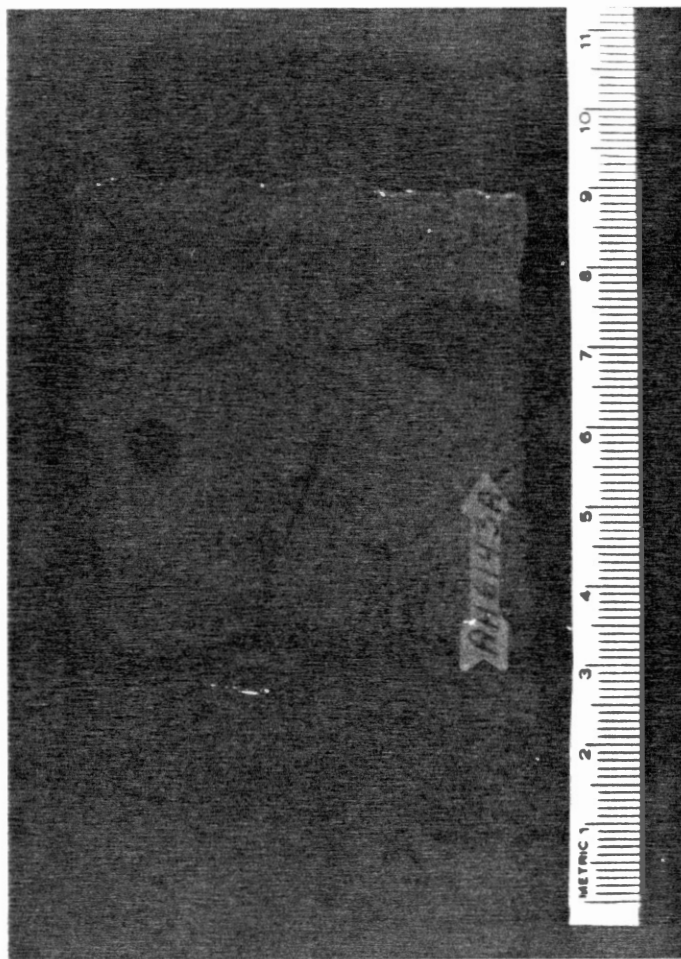


Figure 12. Soft Sediment Flowage,
Honolulu Oil Maben O. 2.
Depth 6143 Ft. Shown on
Arrow

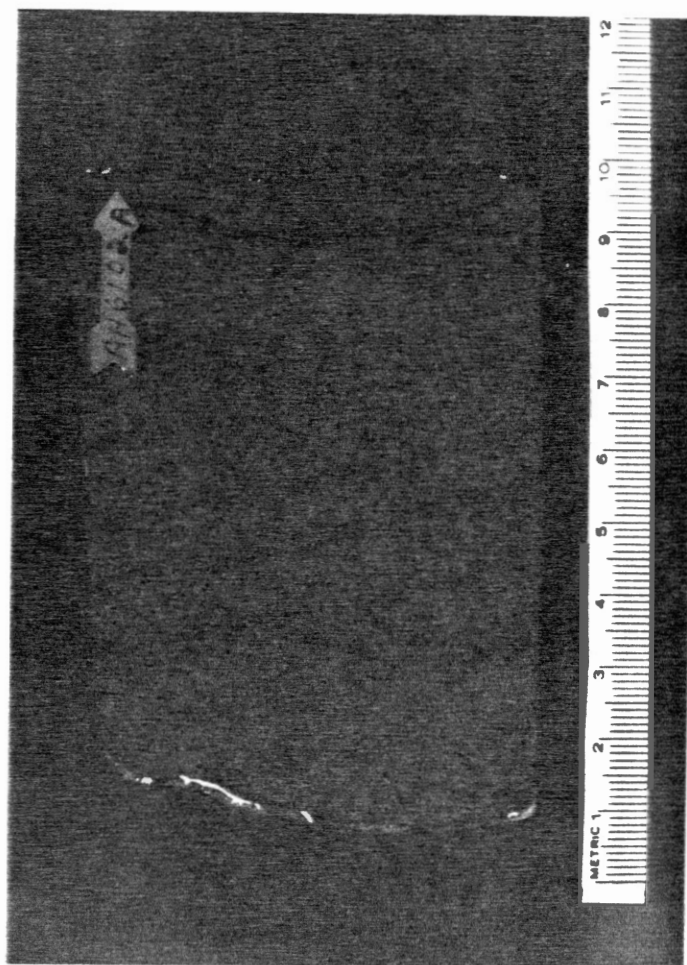


Figure 13. Medium-scale Crossbedding,
Honolulu Oil Maben No. 2.
Depth 6102 Ft. Shown on
Arrow

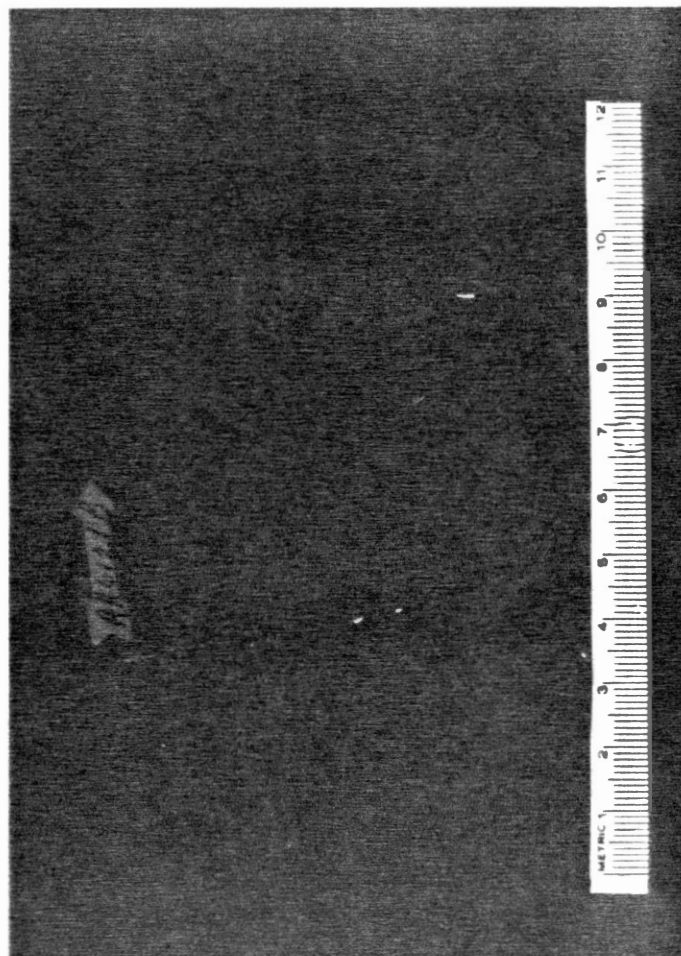


Figure 14. Medium-scale Crossbedding,
Honolulu Oil Newman Bros.
No. 2. Depth 6121 Ft.
Shown on Arrow

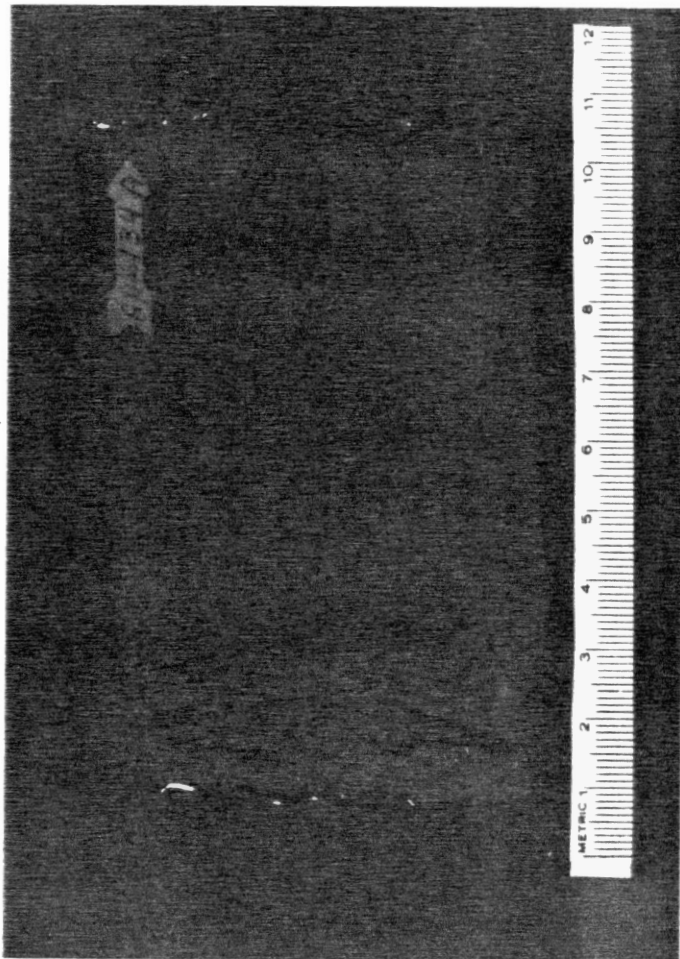


Figure 15. Massive Bedding or Possible Faint, Inclined Lamination, Honolulu Oil Maben No. 2. Depth 6134 Ft. Shown on Arrow. Note the Intraformational Clasts and Apparent Oil-Water Contact

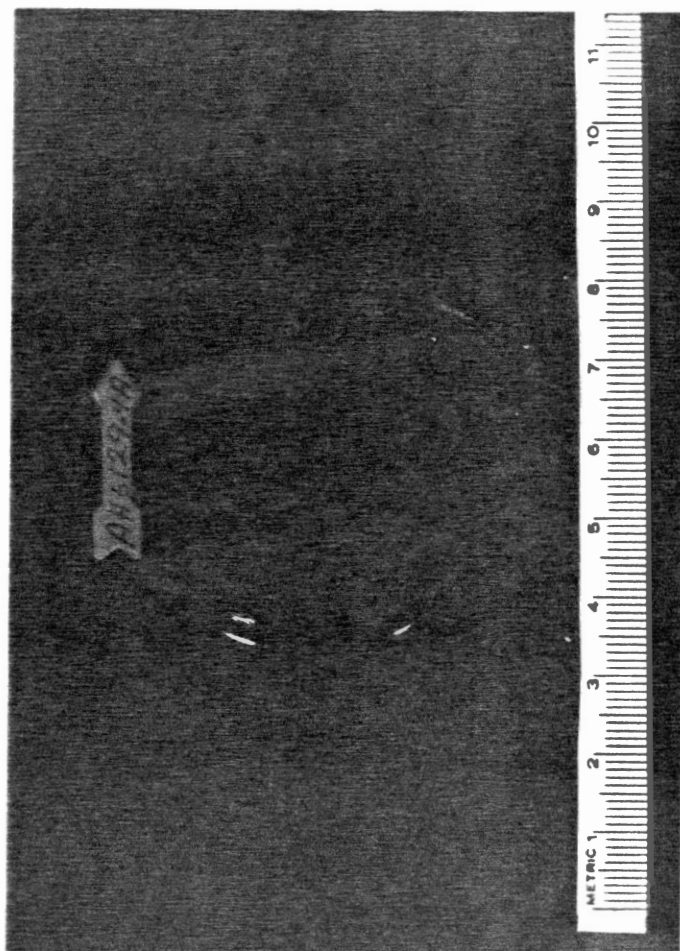


Figure 16. Burrowed-to-Mottled Appearance of Interstratified Sandstone and Shale, Honolulu Oil Maben No. 2. Depth 6129.4 Ft. Shown on Arrow

only significant causes of grain size variation within beds of sandstone. Intraformational conglomerates are uncommon (Figure 17), and the clasts tend to be randomly distributed.

Interstratified sandstone and shale sections change vertically in grain size. Fining-upward from wavy to lenticular ripple-bedding was commonly observed.

Constituents

Major framework grains in the Atkins Sandstone are quartz, feldspar, glauconite, and additional rock fragments. According to the classification proposed by McBride (1963), the Atkins Sandstone at SMS Field is lithic subarkose. (Glauconite was considered to be a rock fragment for the purpose of this classification.)

Quartz is the dominant framework mineral, making up 70 to 80% of the framework. Feldspar is second in abundance, composing 10 to 20% of the framework. Potassium feldspar is slightly more common than plagioclase. Glauconite is third in abundance, making up 4 to 8% of the framework. Additional rock fragments account for 2 to 3% of the framework. Most of these probably represent metamorphic grains. Accessory minerals include muscovite, biotite, chert, zircon, tourmaline, and pyrite.

Fossils were not recognized as a constituent of the Atkins Sandstone. However, within a shale core of the Atkins interval from western Garza County, outside the study area, thin beds of shell and crinoidal debris were recorded.

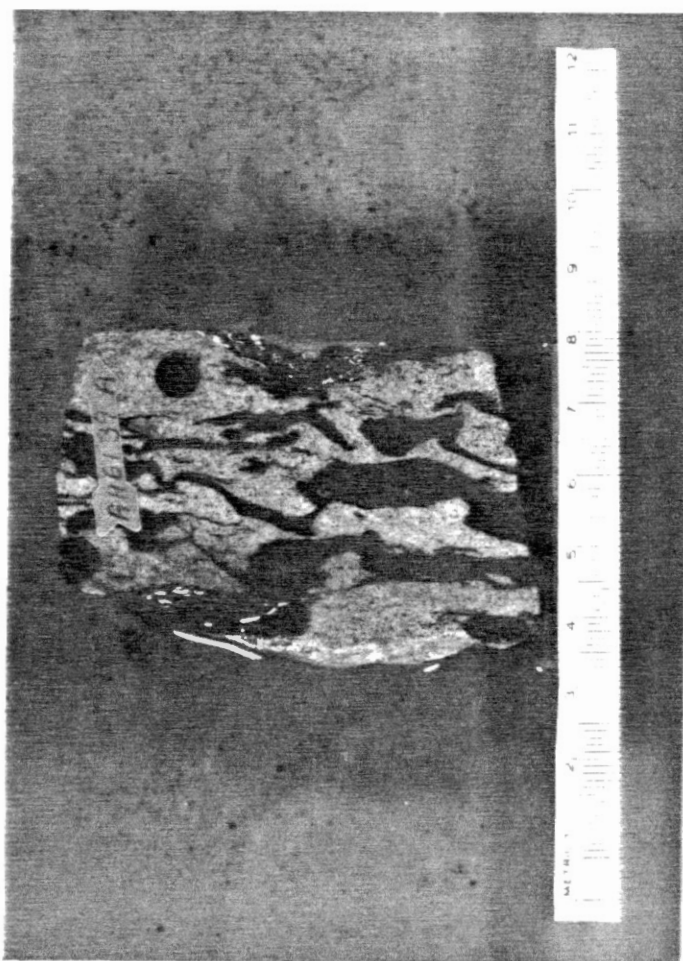


Figure 17. Intraformational Conglomerate,
Honolulu Oil Maben No. 2.
Depth 6139 Ft. Shown on
Arrow

CHAPTER VIII

DEPOSITIONAL ENVIRONMENT

The geometric relationship of the Atkins Sandstone across the study area is suggestive of three separate depositional environments within a given geologic setting. Geologic setting is helpful in eliminating a number of unlikely depositional environments. Electric-log profiles through the Atkins interval resemble the basinal system profiles described in the Palo Duro Basin by Handford and Dutton (1980). Sparse fauna within surrounding shale may imply a deep basinal setting, but sparsity of fauna is representative of conditions at the delta-front also. A basinal setting is consistent with the interpretation by previous investigators who have described the Atkins interval as representing the equivalent of the Pennsylvanian to Permian shelf edges to the east. The maximum dip of the eastern slope has been described as 3° and decreasing basinward. The structural configuration of the "M" zone represents a depositional slope of less than or equal to $.50^{\circ}$.

The paleotopographic surface on which the Atkins interval was deposited is illustrated by Plate 4. Two schematic diagrams (Figures 18 and 19) attempt to present two alternative hypotheses responsible for the topographic relief of this surface. Solution of the origin of the topographic relief is beyond the scope of this study; the limestone rock masses commonly have been referred to as buildups, implying depositional topography, and will be discussed as such in following illustrations.

Sandstone geometry is helpful in approximating reasonable

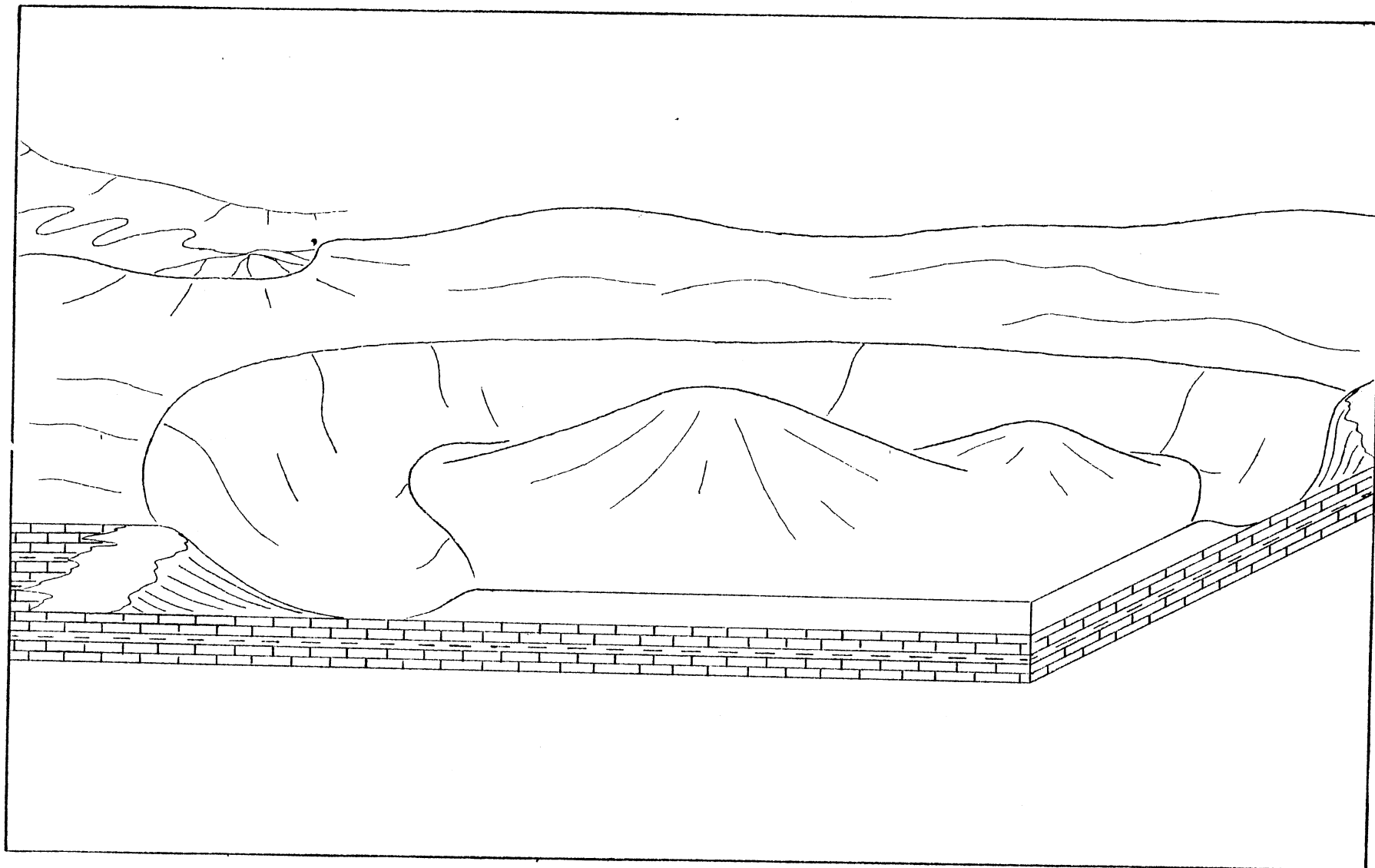


Figure 18. Schematic Diagram of the Study Area Prior to Atkins Sandstone Deposition Portraying Depositional Topography. Note the Reef and Fore-Reef Deposition Along Proposed Shelf Edge

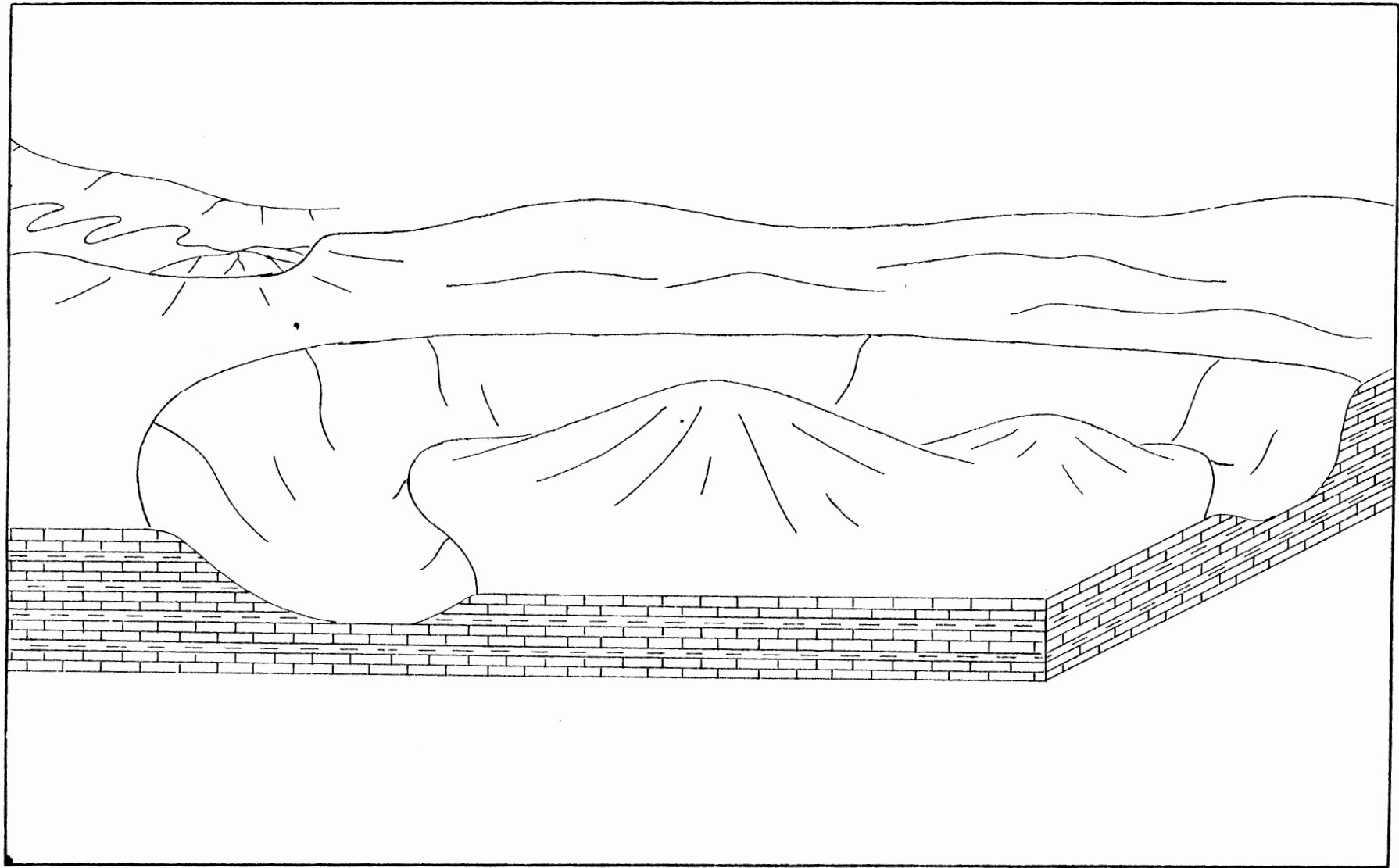


Figure 19. Schematic Diagram of the Study Area Prior to Atkins Sandstone Deposition Portraying Erosional Topography. Note the Truncation of Beds Along Proposed Shelf Edge

depositional environments within the given geologic setting. The geometry of the Atkins "A" Sandstone bears resemblance to sand bars within a shallow marine to delta-front environment. This interpretation is consistent with the environmental interpretation for the stratigraphically equivalent Tannehill Sandstone in Dickens County (Baker, 1975) and the Cook Sandstone (Bloomer, 1977).

The vertical sequence would appear to show distal bars overlain by a distributary-mouth bar complex. The proposed distal bar is less extensive than the overlying distributary-mouth bars and is characterized by a sharp basal contact. The proposed distributary-mouth bars are widespread along the northern edge of the Lower Strawn platform. The basal contacts appear gradational, and laterally the sandstone interfinger with the surrounding shales. Coarsening upward of grain size is assumed from spontaneous-potential curve profiles.

The Atkins "B" Sandstone geometry is that of a channel. The lower and lateral contacts are sharp, and the boundary of the flat upper surface is moderately sharp. The channel overlies the Atkins "A" Sandstone in the northern part of the study area. Two reasonable environments can be suggested for the genesis of the channel: (1) it represents a deltaic distributary related to the proposed underlying delta-front sediments, or (2) it represents a marine channel that transported an excess of clastic material downslope from the delta-front terrain.

Basinward the channel thickens dramatically into a clastic wedge. Distributary-mouth bars would be present basinward of a deltaic distributary, whereas marine fans would exist basinward of a marine channel. The sharp lower contact would suggest a lack of reworking by

wave action, and would support a more basinward interpretation.

Rock data are limited to the Atkins "B" Sandstone at SMS Field. The internal features observed should be helpful in differentiating between a deltaic distributary versus a marine channel. The majority of primary sedimentary structures are current generated, which is to be expected in either environment. The sedimentary structures do not form a diagnostic vertical sequence characteristic of a distributary environment. The uniform grain size is unlike the fining-upward sequences of deltaic distributaries. Sand deposition appears to have occurred as rapid, discrete pulses. The abundance of intercalated shales suggests that the introduction of sand interrupted deposition of clay. The abundance of flowage and loading is suggestive of deformation subsequent to rapid sand deposition.

Detrital constituents are generally most useful in providing information concerning provenance, but because glauconite consists of as much as 8% of the framework, composition may be environmentally significant, and is suggestive of a marine influence.

The amount of feldspar in the Atkins "B" Sandstone is suggestive of an igneous source area. The presence of zircon and tourmaline in trace amounts support this suggestion. The Amarillo-Wichita uplift would seem to be the most likely source area considering the regional slope and proximity to the study area.

The proposed depositional model for the Atkins Sandstone requires two major stages of deposition. The first stage accompanied Atkins "A" Sandstone deposition along the northern edge of the Lower Strawn platform as sand bars in a shallow marine to delta-front environment (Figure 20). Initial shale deposition within the lower Atkins interval

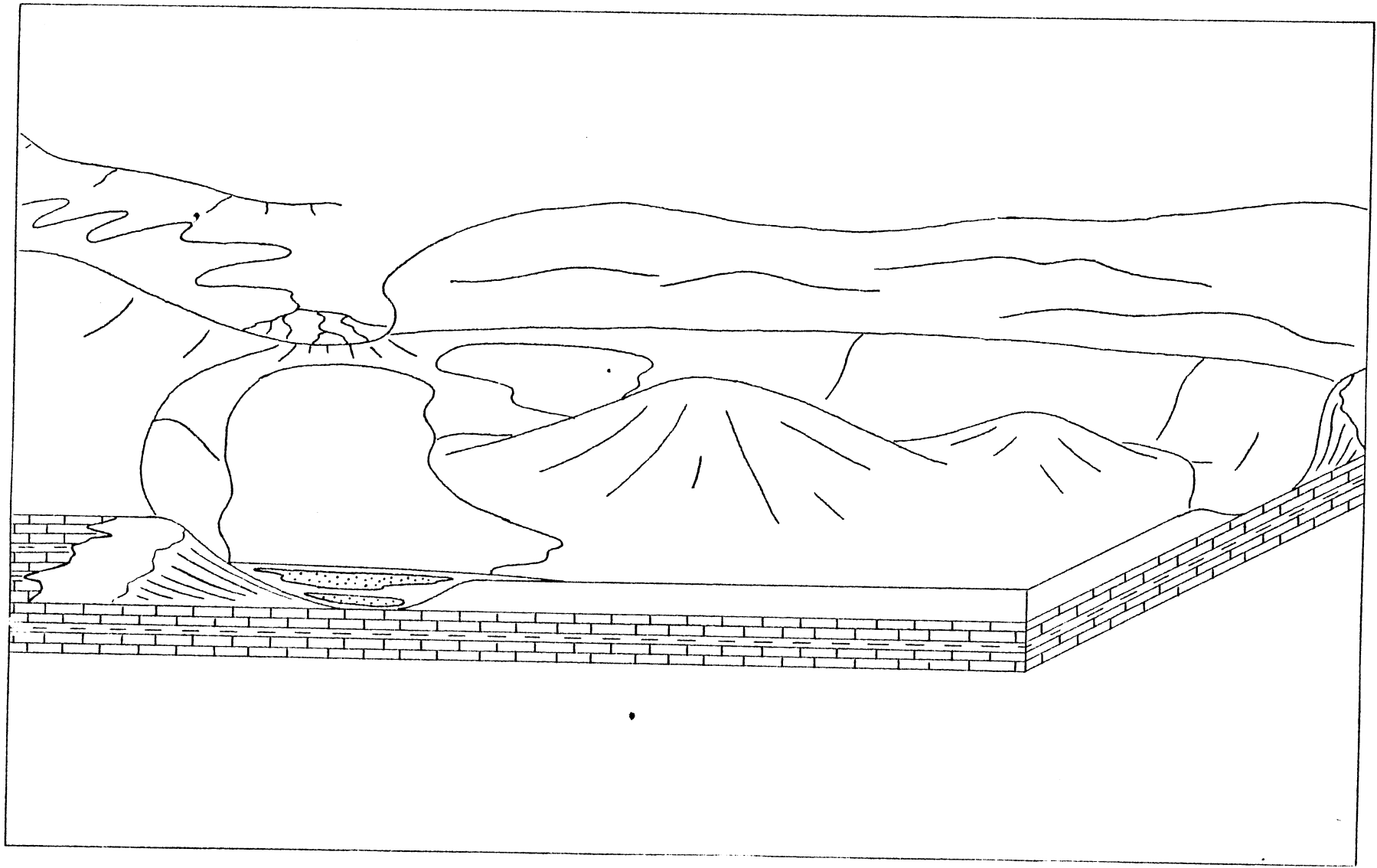


Figure 20. Schematic Diagram of the Study Area Subsequent to Atkins "A" Sandstone Deposition, but Prior to Atkins "B" and "C" Sandstone Deposition

probably occurred across the entire study area during this stage. The second stage accompanied deposition of Atkins "B" and "C" Sandstone as marine channel and fan deposits as excess sand was distributed over the Lower Strawn platform (Figure 21).

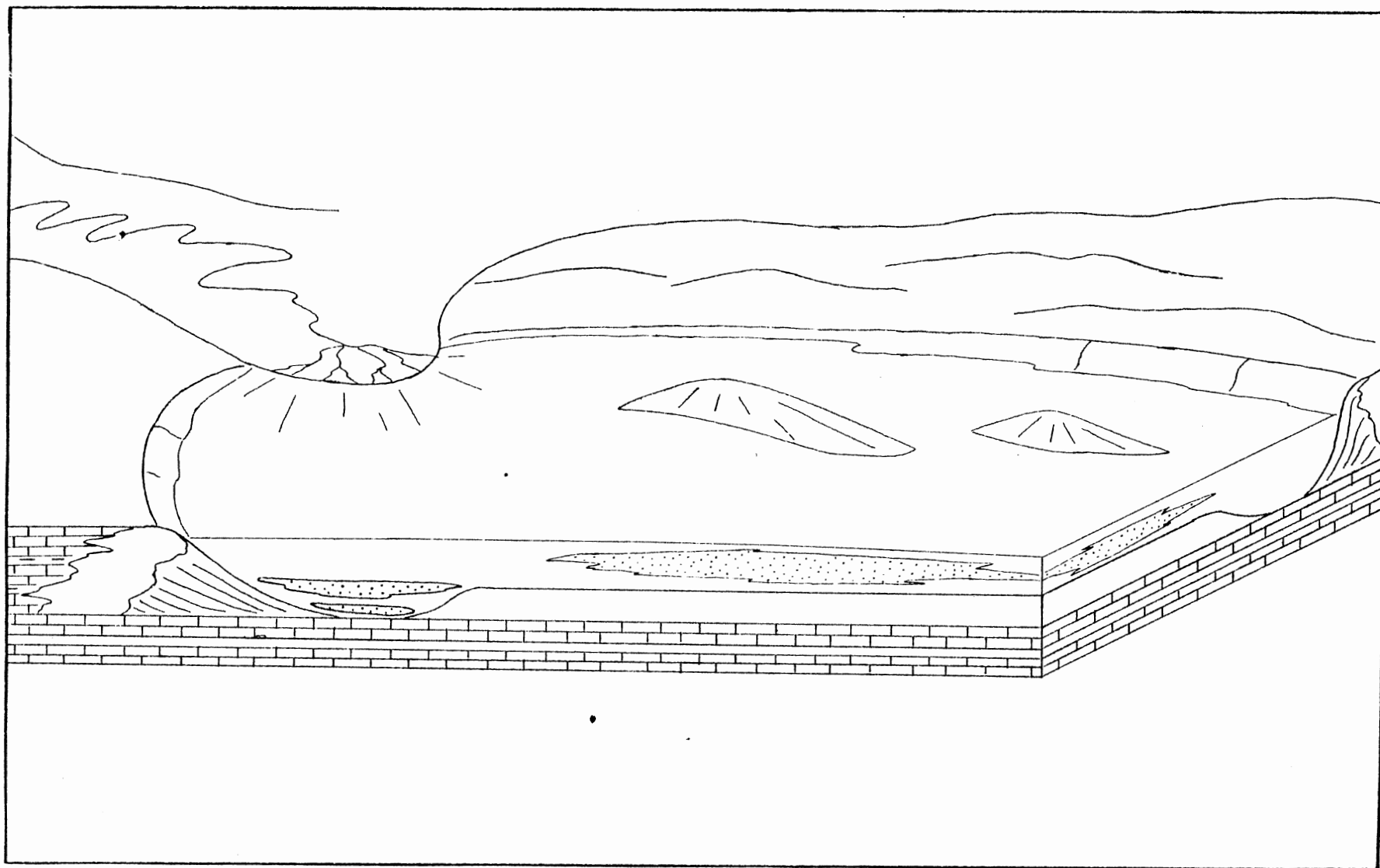


Figure 21. Schematic Diagram of the Study Area Subsequent to Atkins "B" and "C" Sandstone Deposition

CHAPTER IX

DIAGENESIS OF THE ATKINS SANDSTONE

Diagenesis of the Atkins Sandstone consists of at least ten post-depositional changes. Though the exact order is unknown, the events will be discussed in the approximate order of occurrence through three principal stages.

Stage 1: The initial stage consists of changes which contributed to the reduction of primary intergranular porosity. Precipitation of silica along quartz grain boundaries is evident as sytaxial quartz overgrowths (Figure 22). The plasticity of rock fragments (including glauconite grains) resulted in squeezing of these grains into adjacent pore spaces, forming a pseudomatrix (Figures 23 and 24). Compaction along carbonaceous shale laminae resulted in the generation of pyritized stylolites. Precipitation of calcite cement accompanied the corrosion of quartz grains and overgrowths. In most of the thin sections the calcite cement is patchy in occurrence (Figure 23), whereas in tight streaks it is more abundant (Figure 25).

Stage 2: The second stage consists of alteration and in some cases dissolution of unstable constituents. Glauconite grains have been altered to the iron-deficient clay mineral (illite). Altered glauconite grains are yellowish brown (Figure 23), whereas a few unaltered grains have remained green. Additional rock fragments, probably metamorphic grains, have been altered to sericite (Figure 23). Calcite cement has been altered to iron-rich dolomite or ankerite (Figure 25). It would

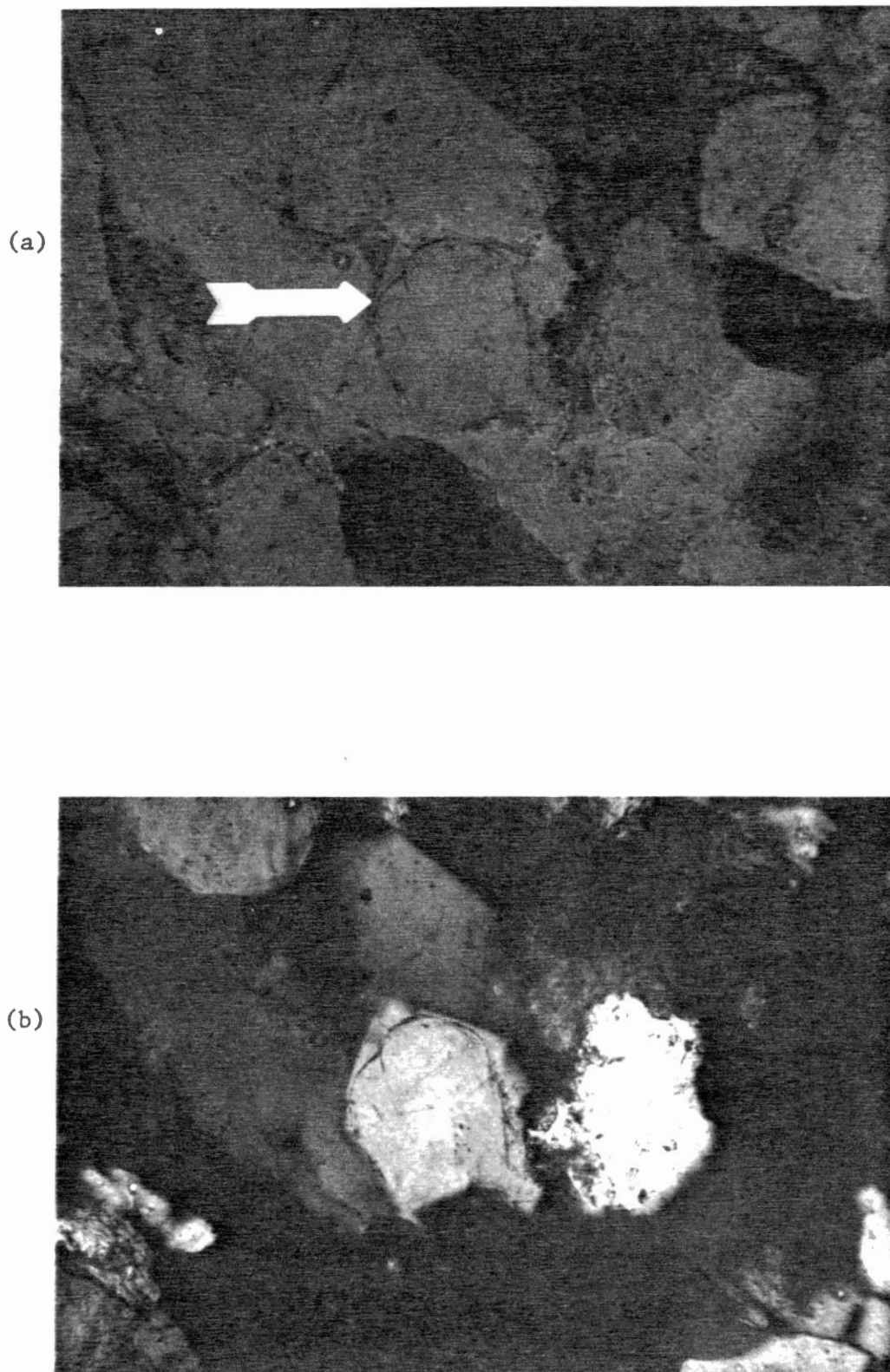


Figure 22. Syntaxial Quartz Overgrowth Shown by Obvious Pre-Overgrowth Grain Boundary, Magnification 100X. (a) Plane-Polarized Light. (b) Crossed-Nicols. Sample From Honolulu Oil Maben No. 2, Depth 6145 Ft.

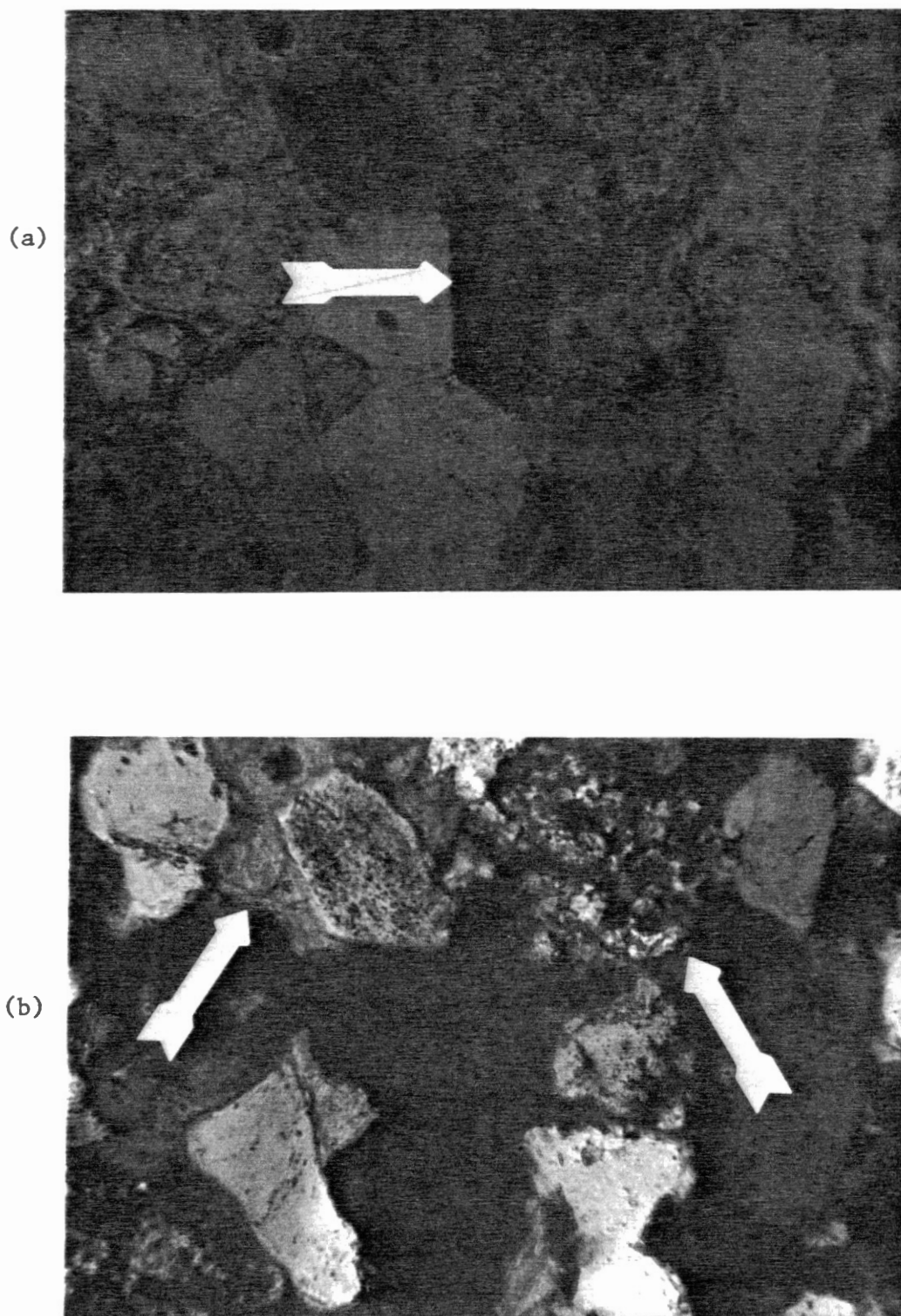


Figure 23. Glauconite Grain Altered to Iron-Deficient Clay. Note the Grain is Squeezed Into Adjacent Pores Forming a Pseudomatrix. Magnification 100X. (a) Plane-Polarized Light. (b) Crossed-Nicols. Note the Grain Altered to Sericite and the Ankerite Cement. Sample From Honolulu Oil Maben No. 2, Depth 6125.5 Ft.

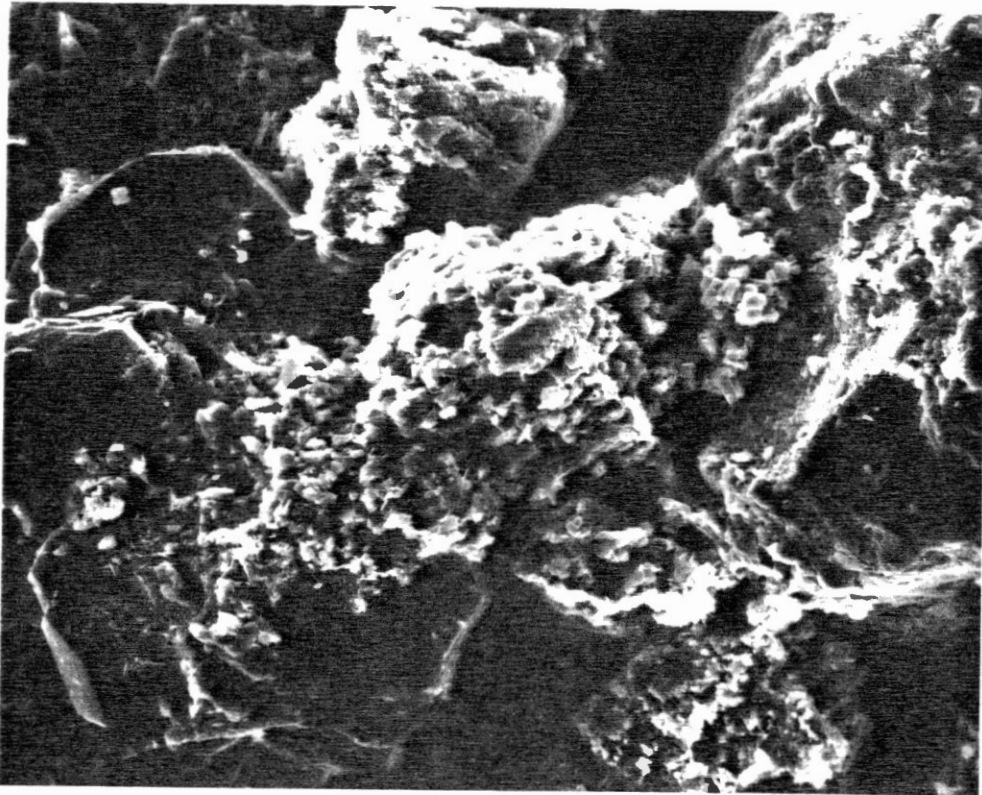


Figure 24. Glauconite Pseudomatrix. Magnification 200X.
Sample From Honolulu Oil Maben No. 2, Depth
6102 Ft.

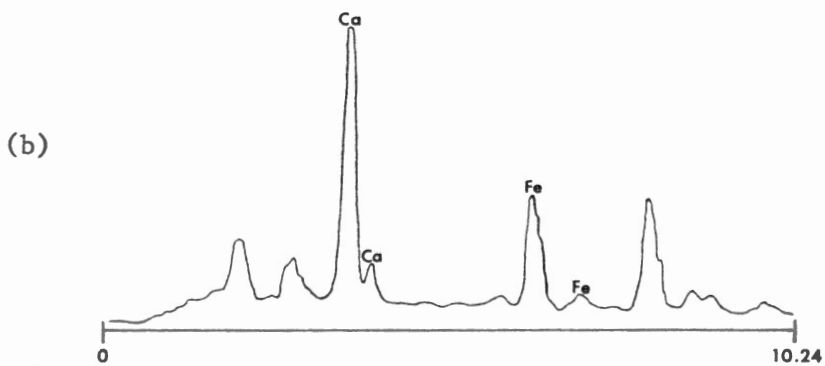
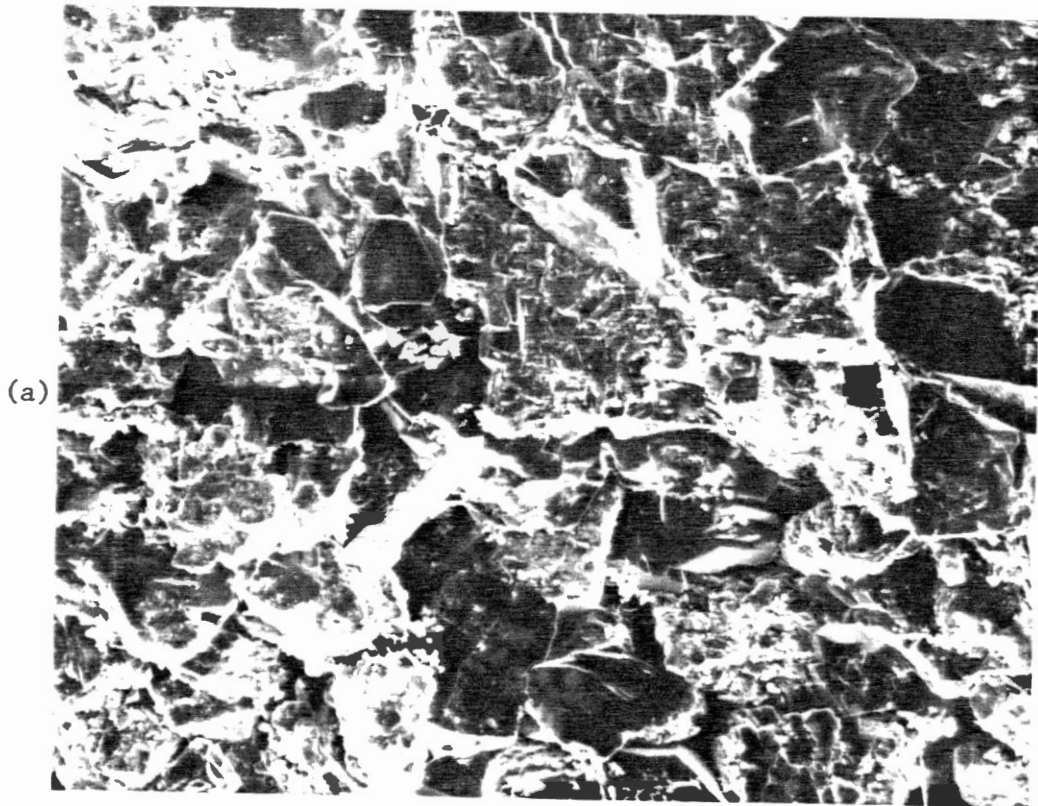


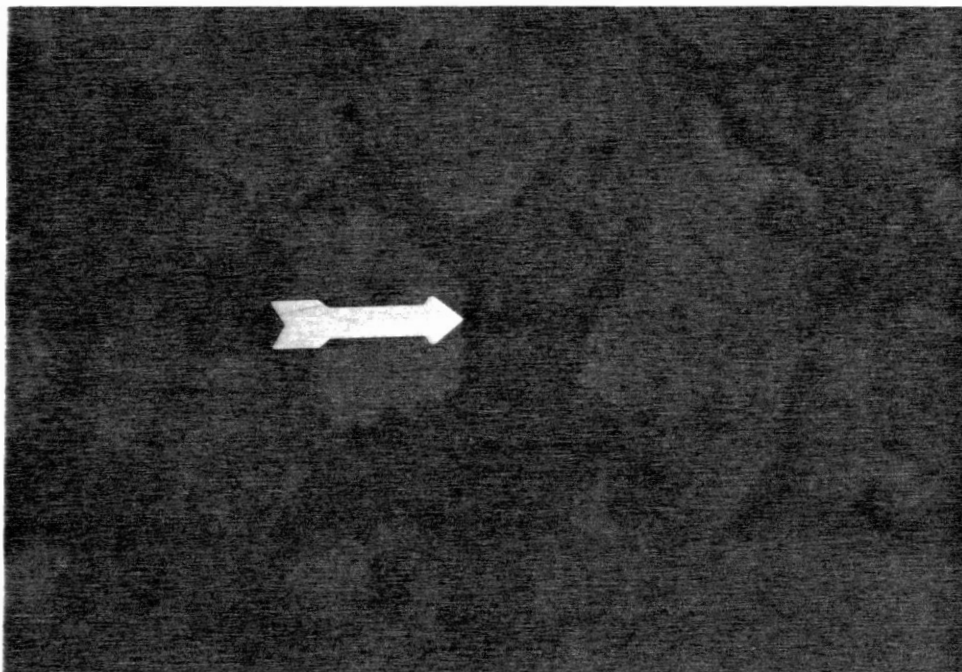
Figure 25. (a) Ankerite Cement. Magnification 100X.
(b) Energy Dispersive X-ray Analysis
Showing Evidence of Substitution. Sample
From Honolulu Oil Maben No. 2, Depth
6145 Ft.

seem reasonable that the alteration of calcite accompanied or occurred subsequent to the alteration of glauconite, which would provide a source of iron.

Secondary porosity is very common in the Atkins Sandstone; e.g., the presence of oversized pores and partially dissolved grains of feldspar (Figures 26 and 27). Floating quartz grains with corroded grain boundaries (Figure 26) also suggest possible dissolution of prior carbonate cement.

Stage 3: Precipitation of authigenic clay minerals appears to have been the final stage of diagenesis. Vermicular kaolinite (Figure 28) as partial pore fillings and chlorite (Figure 29) as pore linings are most obvious. Energy dispersion X-ray analysis demonstrates the substitution of iron into the chlorite structure (Figure 30). Mixed-layer clays and illite are minor cementing agents in the Atkins Sandstone.

(a)



(b)



Figure 26. Partially Dissolved Feldspar Grain (Center) Forming Secondary Porosity. Note the Dissolution Along Cleavage, Magnification 100X. (a) Plane-Polarized Light. (b) Crossed-Nicols. Sample From Honolulu Oil Maben No. 2, Depth 6145 Ft.

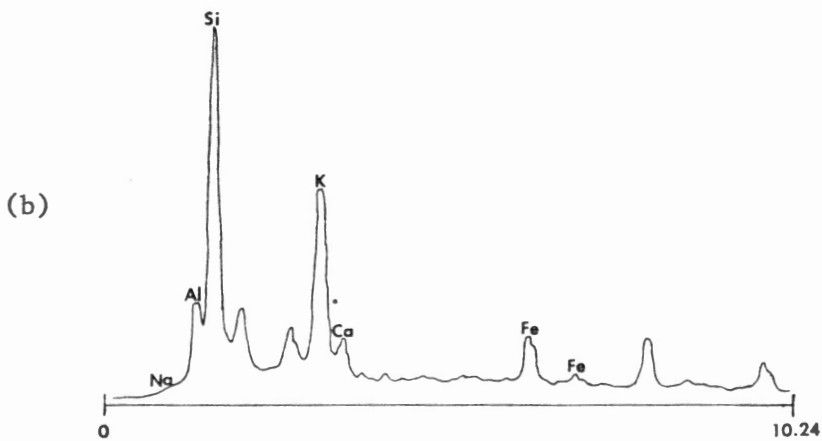
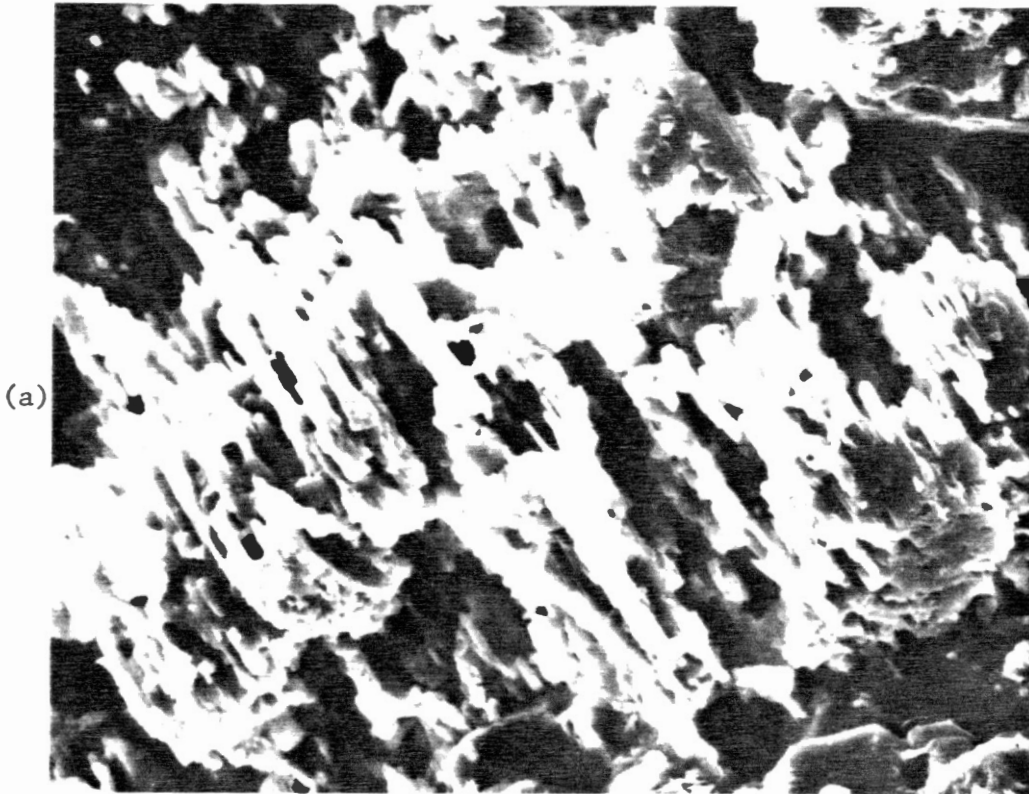


Figure 27. (a) Partially Dissolved Feldspar Grain. Magnification 400X. (b) Energy Dispersive X-ray Analysis Indicating That the Grain is Potassium Feldspar. Sample From Honolulu Oil Maben No. 2, Depth 6141 Ft.

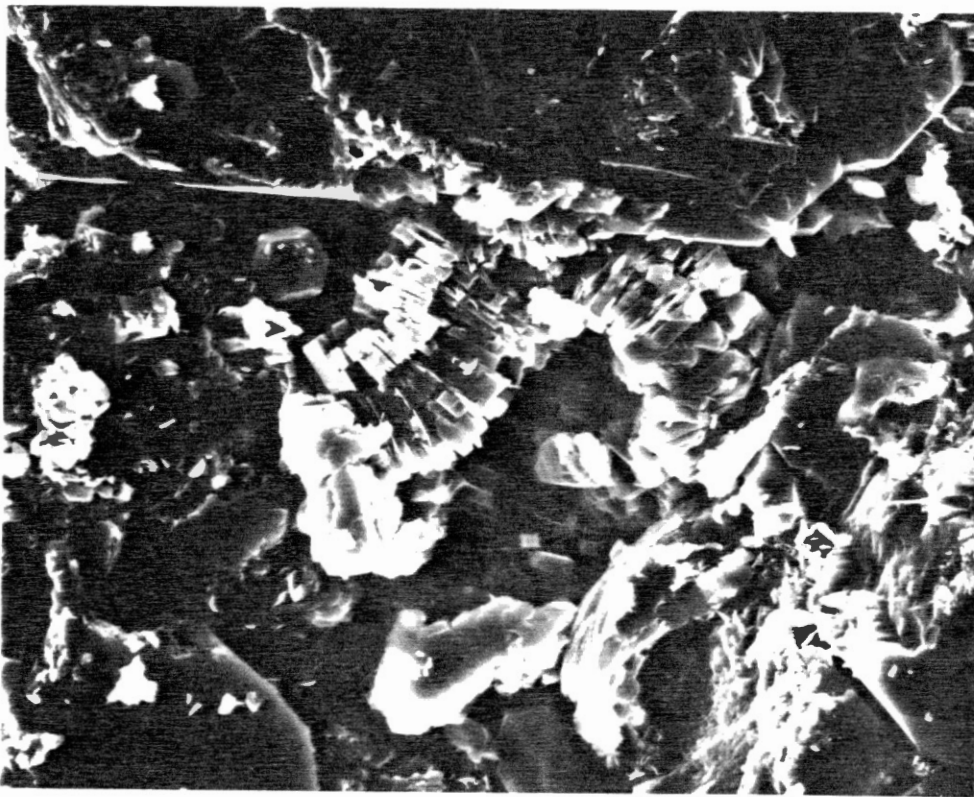


Figure 28. Vermicular Kaolinite Partially Filling Pore,
Magnification 400X, Sample From Honolulu
Oil Maben No. 2, Depth 6122 Ft.

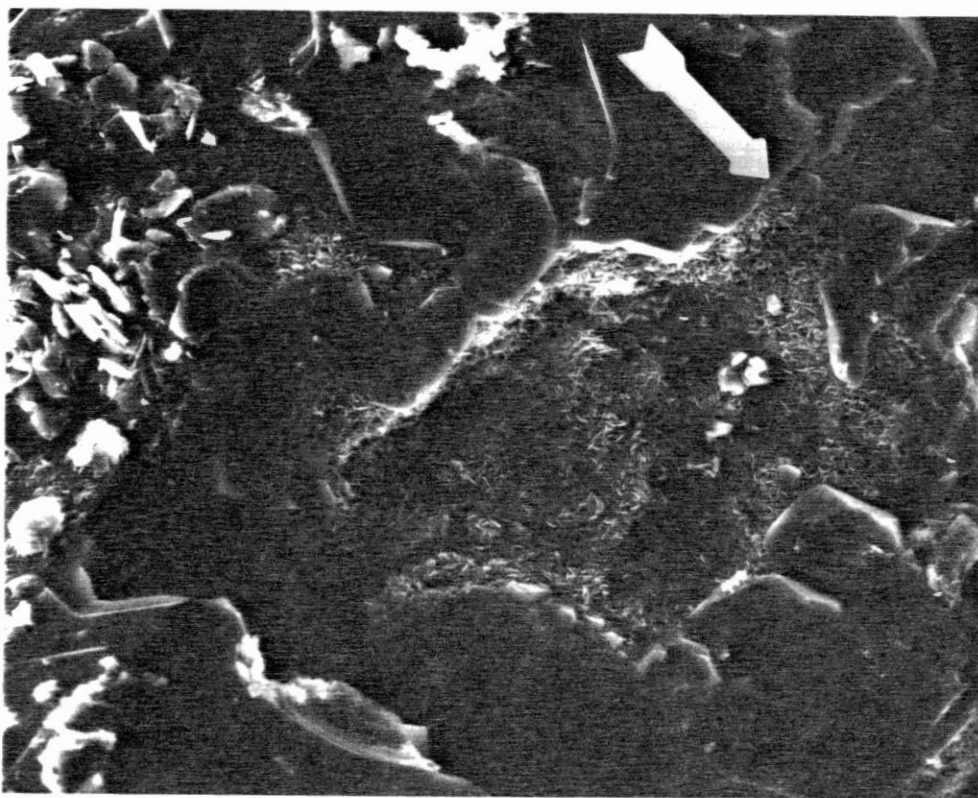


Figure 29. Chlorite Lining Pore. Note the Continuity of the Clay Lining Through the Pore Throat. Magnification 400X. Sample From Honolulu Oil Maben No. 2, Depth 6141 Ft.

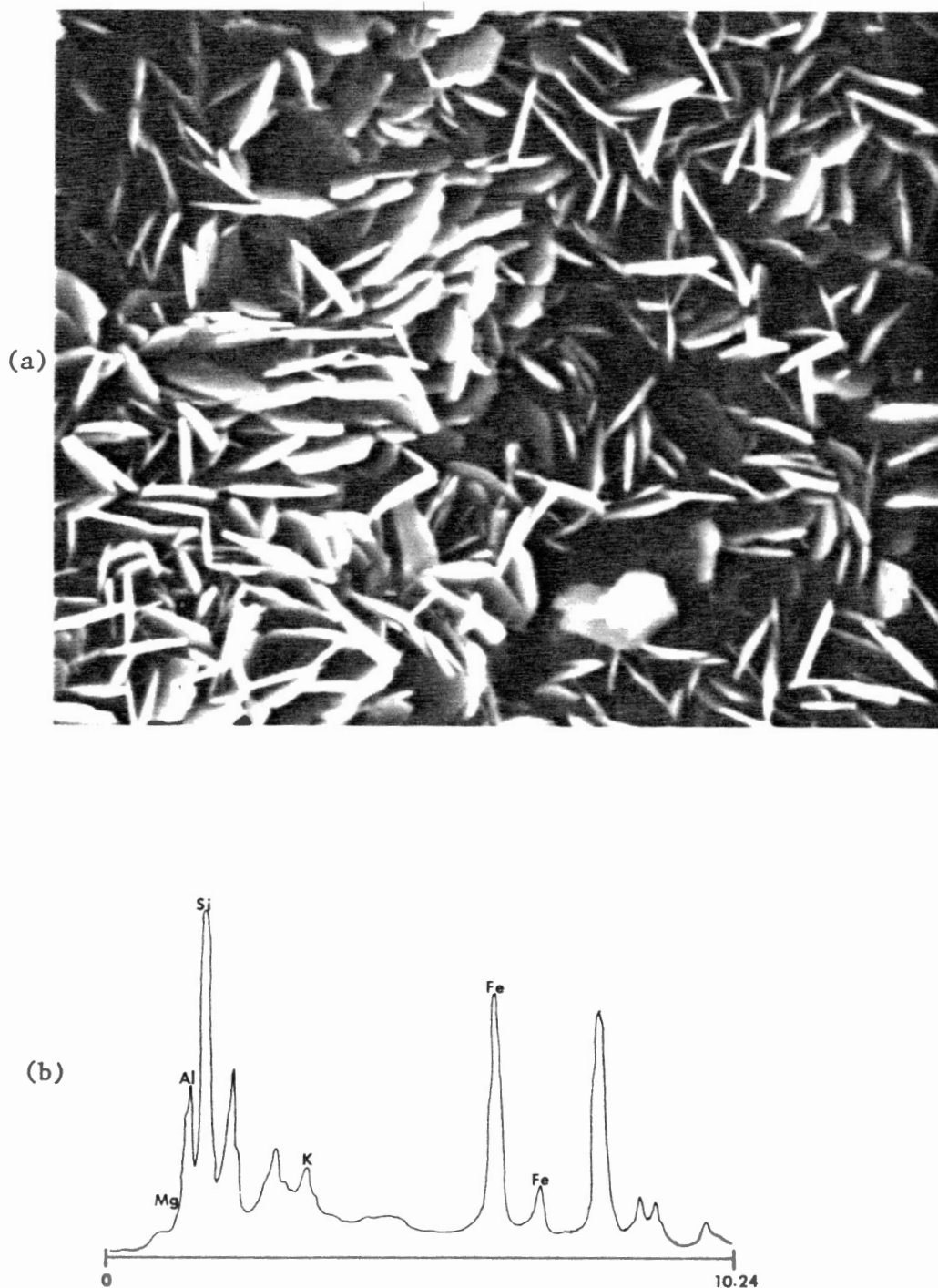


Figure 30. (a) Chlorite Lining Pore. Note the Micro-Porosity. Magnification 2000X. (b) Energy Dispersive X-ray Analysis Illustrating Almost Complete Iron Substitution. Sample From Honolulu Oil Maben No. 2, Depth 6141 Ft.

CHAPTER X

PORE GEOMETRY

Intergranular, secondary, micro-, and fracture porosity are present in the Atkins Sandstone at SMS Field. Secondary and micro-porosity are most common, and fracture porosity occurs only as a trace. The sandstone in SMS Field has an average porosity of 19% and average permeability of 117 md.

Intergranular porosity was reduced greatly during stage 1 of diagenesis. Small pore openings adjacent to non-corroded syntaxial quartz overgrowths (Figure 22) suggest that porosity was not totally eliminated. The total volume associated with the intergranular porosity may be small, but these pore openings serve to interconnect other pore types, thus increasing permeability.

Secondary porosity accounts for the majority of total porosity. It ranges from small cracks along the cleavage of partially dissolved feldspar grains to total dissolution of previously introduced grains and cement.

Micro-porosity occurs dominantly between chlorite platelets (Figure 30) but also occurs between kaolinite platelets (Figure 28) and partially dissolved feldspar grains (Figure 27). The precipitation of authigenic chlorite significantly increased the total surface area within the Atkins Sandstone, probably without significantly reducing the total porosity. Two water layers bound to the surface area adjacent to clay surfaces represents that part of the true water saturation which is

irreducible. Bound water also increases the ionic concentration of the reducible water within the reservoir, which tends to increase the apparent water saturation derived from well-log analyses. The net result creates a tendency to underestimate the quality of a potential reservoir.

CHAPTER XI

APPLICATIONS OF INVESTIGATION

Practical applications of this study are confined mostly to exploration and production of hydrocarbons within the Atkins Sandstone and similar sandstone bodies.

The trapping mechanism for SMS and White River Fields is combination-structural and stratigraphic. These pools accumulated within channel-type sandstone bodies trending roughly along regional strike. SMS and White River Fields occur where the channel trend crosses a structural nose (Plates 3 and 5) (Figure 2). Updip meander loops in such channels would also be sufficient in creating a trapping situation.

To date, production has been discovered only in channel-type sandstone bodies in the study area, trapping within any sandstone body with an abrupt up-dip termination would seem to be reasonably probable. The eastern limit of Garza and Kent Counties are circumstances of this basic type.

Diagenesis of the Atkins Sandstone is closely associated with several applications to exploration and production. Development of micro-porosity between authigenic clay platelets results in formational water being irreducibly bound to the reservoir. Water saturation calculations for productive intervals at SMS Field yielded mid-range calculations (S_w 50%), yet water-free initial production in excess of 100 bbls. per day was accomplished. The discovery well for SMS Field,

originally abandoned, was subsequently re-entered and completed as an oil well. Good well-site techniques become increasingly important when dealing with this reservoir type.

The types of authigenic clays present are both associated with production problems. Kaolinite is typically attached rather loosely to host grains. High fluid turbulence, especially close to the well bore, can detach kaolinite particles, allowing them to migrate to the pore throats. Clay stabilization, such as the introduction of polyhydroxy aluminum, if carried out early in the history of such a well, will help prevent such migration of fines.

Chlorite is extremely sensitive to acid and oxygenated waters. Iron-rich chlorite, such as that in the Atkins Sandstone, will liberate iron during dissolution. Free iron may then reprecipitate as a gelatinous ferric hydroxide when the acid is spent. If acidization is desirable, an oxygen scavenger and an iron-chelating agent should be included in the treatment. It is also important to recover the full load introduced into the interval being treated without significant delays. The same precautions should be observed when dealing with ankerite cement, which is also present within the Atkins Sandstone.

CHAPTER XII

SUMMARY

The principal conclusions of this investigation are:

1. The geologic setting of the Atkins interval across the study area is a basinal setting on the northeastern slope of the Midland Basin.
2. The Atkins interval is roughly equivalent to the stratigraphic interval on the eastern shelf between the Saddle Creek Limestone and Crystal Falls Limestone.
3. Thickness of the Atkins Sandstone is directly related to the thickness of the Atkins interval, basinward to the point of maximum sandstone thickness.
4. The sandstone distribution and depositional environment were influenced by the topographic relief of the Pennsylvanian limestone surface on which the Atkins interval was deposited.
5. Delta-front to shallow marine environments were present along the northern and northeastern edges of the Lower Strawn platform.
6. Sand was distributed over the Lower Strawn platform adjacent to Swenson and Salt Creek buildups as marine channels and fans.
7. Composition of the Atkins Sandstone and regional slope of the geologic setting suggest that the Wichita-Amarillo uplift was the major source area.
8. Original intergranular porosity of the Atkins Sandstone was reduced greatly by compaction and cementation.

9. Dissolution of unstable constituents produced well developed secondary porosity.

10. Precipitation of clay minerals as pore fillings and grain coatings produced micro-porosity and significantly increased surface areas adjacent to porosity, but probably did not significantly reduce the total porosity.

11. The possibility of future oil discoveries within the Atkins interval is promising along the trend of abrupt up-dip sandstone limits.

12. Productivity of sandstone within the Atkins interval cannot be analyzed accurately merely by water-saturation calculations.

13. Once the feasibility of a production test has been established within the Atkins Sandstone, authigenic components should be identified and production techniques planned accordingly.

SELECTED REFERENCES

- Adams, J. E., Frenzel, H. N., Rhodes, M. L., and Johnson, D. P., 1951, Starved Pennsylvanian Midland Basin: Am. Assoc. Petroleum Geologists Bull., v. 35, p. 2600-2607.
- Al-Shaieb, Z., and Shelton, J. W., 1978, Secondary ferroan dolomite rhombs in oil reservoirs, Chadra Sands, Gialo Field, Libya: Am. Assoc. Petroleum Geologists Bull., v. 62, p. 463-468.
- Almon, W. R., Fullerton, L. B., and Davies, D. K., 1976, Pore space reduction in Cretaceous sandstones through chemical precipitation of clay minerals: Jour. Sed. Petrol., v. 46, p. 89-96.
- Asquith, D. O., 1970, Depositional topography and major marine environments, Late Cretaceous, Wyoming: Am. Assoc. Petroleum Geologists Bull., v. 54, p. 1184-1224.
- Baker, H., 1975, Confidential Amoco report.
- Ball, S. M., and Short, M., 1979, Confidential Amoco report.
- Bloomer, R. R., 1977, Depositional environments of a reservoir sandstone in west-central Texas: Am. Assoc. Petroleum Geologists Bull., v. 61, p. 344-359.
- Brown, L. F., Jr., 1969, Geometry and distribution of fluvial and deltaic sandstones (Pennsylvanian and Permian), north-central Texas: Gulf Coast Assoc. Geol. Soc. Trans., v. 19, p. 23-47.
- Burnside, R. J., 1959, Geology of part of the Horseshoe Atoll in Borden and Howard Counties, Texas: U.S. Geol. Survey Prof. Paper 315-B.
- Busch, D. A., 1974, Stratigraphic traps in sandstone - exploration techniques: Am. Assoc. Petroleum Geologists Memoir 21, 174 p.
- Cartwright, L. D., Jr., 1930, Transverse section of Permian Basin, west Texas and southeast New Mexico: Am. Assoc. Petroleum Geologists Bull., v. 14, p. 969-981.
- Cheney, M. G., 1918, Economic importance of the Bend Series in north-central Texas as a source of petroleum supply: Oil Trade Jour., v. 9, April, p. 109-110.
- _____, 1929, History of the Carboniferous sediments of the Mid-Continent oil field: Am. Assoc. Petroleum Geologists Bull., v. 13, p. 557-594.

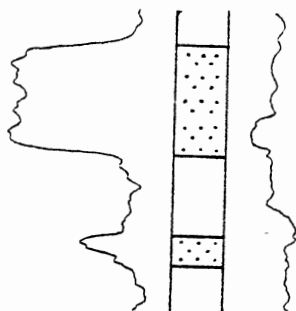
- Davies, D. K., and Ethridge, F. G., 1975, Sandstone composition and depositional environment: Am. Assoc. Petroleum Geologists Bull., v. 59, p. 239-264.
- Galley, J. E., 1955, Oil and geology in the Permian Basin of Texas and New Mexico: Habitat of oil--A symposium: conducted by Am. Assoc. Petroleum Geologists; p. 395-446.
- Galloway, W. E., and Brown, L. F., 1972, Depositional systems and shelf-slope relationships in Upper Pennsylvanian rocks, north-central Texas: Am. Assoc. Petroleum Geologists Bull., v. 61, p. 1437-1447.
- Gould, C. N., and Lewis, F. E., 1926, The Permian of western Oklahoma and the panhandle of Texas: Okla. Geol. Survey Circ. No. 13.
- Grim, R. E., 1968, Clay mineralogy: McGraw-Hill, New York, 596 p.
- Handford, C. R., and Dutton, S. P., 1980, Pennsylvanian-Early Permian depositional systems and shelf-margin evolution, Palo Duro Basin, Texas: Am. Assoc. Petroleum Geologists Bull., v. 64, p. 88-106.
- Hein, J. R., Allwardt, A. O., and Griggs, G. B., 1974, The occurrence of glauconite in Monterey Bay, California; diversity, origins, and sedimentary environmental significance: Jour. Sed. Petrology, v. 44, p. 562-571.
- Jones, T. S., 1953, Stratigraphy of the Permian Basin of West Texas: Special Publication of West Texas Geological Soc., 63 p.
- Krauskopf, K. B., 1979, Introduction to geochemistry: McGraw-Hill, New York, 617 p.
- Lewis, F. E., 1941, Position of San Andreas Group, West Texas and New Mexico: Am. Assoc. Petroleum Geologists Bull., v. 25, p. 73-103.
- McBride, E. F., 1963, Classification of common sandstones: Jour. Sed. Petrology, v. 33, p. 664-669.
- Moorhouse, W. W., 1959, The study of rocks in thin section: Harper and Row, New York, 514 p.
- Pettijohn, F. J., 1975, Sedimentary rocks: Harper and Row, New York, 628 p.
- Reinecke, H. E., and Single, I. B., 1973, Depositional sedimentary environments: Springer-Verlag, New York, Heidelberg, Berlin, 435 p.
- _____. and Wunderlich, F., 1968, Classification and origin of flaser and lenticular bedding: Sedimentology, v. 11, p. 99-105.
- Schmidt, V., and McDonald, D. A., 1979, The role of secondary porosity in the course of sandstone diagenesis, in Schoile, P. A. and

- Schluger, P. R. (eds.), Aspects of diagenesis: Soc. Econ. Paleontologists and Mineralogists Spec. Publ. No. 26, p. 175-207.
- Sellards, E. H., 1934, Major structural features of Texas, east of Pecos River: Texas Univ. Bull. 3401, p. 11-135.
- Selley, R. C., 1970, Ancient sedimentary environments: Chapman and Hall, Ltd., London, 237 p.
- Shelton, J. W., 1973, Models of sand and sandstone deposits: Okla. Geol. Survey Bull. 118, 122 p.
- Stafford, P. T., 1959, Geology of part of the Horseshoe Atoll in Scurry and Kent Counties, Texas: U.S. Geol. Survey Prof. Paper 315-A.
- Totten, R. B., 1954, Palo Duro Basin, Texas: Am. Assoc. Petroleum Geologists Bull., v. 38, p. 2049-2051.
- Van Sicken, D. C., 1958, Depositional topography - examples and theory: Am. Association Petroleum Geologists Bull., v. 42, p. 1897-1913.
- Vertrees, C. D., 1953, Developments in West Texas and southeastern New Mexico: Am. Assoc. Petroleum Geologists Bull., v. 37, p. 1358-1375.
- Visher, G. S., 1965, Use of vertical profile in environmental reconstruction: Am. Assoc. Petroleum Geologists Bull., v. 49, p. 41-61.
- Willis, R., 1929, Preliminary correlation of the Texas and New Mexico Permian: Am. Assoc. Petroleum Geologists Bull., v. 13, p. 997-1030.
- Wilson, J. L., 1975, Carbonate facies in geologic history: Springer-Verlag, New York, Heidelberg, Berlin, 471 p.
- Wilson, M. D., and Pittman, E. D., 1977, Authigenic clays in sandstones: recognition and influence on reservoir properties and paleo-environmental analysis: Jour. Sed. Petrology, v. 47, p. 3-31.

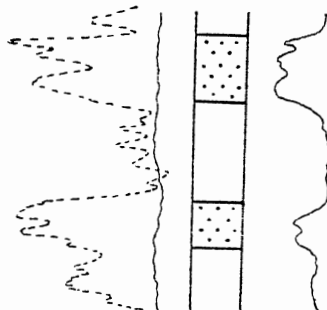
APPENDIX

CRITERIA FOR DETERMINING SANDSTONE BED

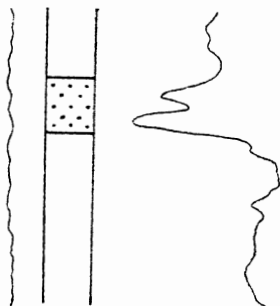
BOUNDARIES ON ELECTRIC LOGS



Case 1: Spontaneous-potential curve is well developed. Bed boundaries picked at inflection-point of a negative SP curve deflection.



Case 2: Spontaneous-potential curve is not developed, and gamma-ray log is available. Bed boundaries picked between inflection-points of a less-counts-per-second gamma-ray deflection and a decreased resistivity deflection.



Case 3: Spontaneous-potential curve is not developed, and gamma-ray log is not available. Bed boundaries picked at inflection-points of a decreased resistivity deflection.

VITA

Gregory R. Simmons

Candidate for the Degree of

Master of Science

Thesis: DEPOSITIONAL ENVIRONMENTS AND DIAGENESIS OF THE ATKINS SANDSTONE, PENNSYLVANIAN TO PERMIAN, NORTHEASTERN MIDLAND BASIN

Major Field: Geology

Biographical:

Personal Data: Born in Bastrop, Louisiana, April 8, 1956, the second son of Mr. and Mrs. Raymond E. Simmons.

Education: Graduated from Northeast High School, Oklahoma City, Oklahoma, in May, 1974; received Bachelor of Science degree in Geology from Oklahoma State University in December, 1978; completed requirements for Master of Science degree at Oklahoma State University in July, 1982.

Professional Experience: Past Junior Member of American Association of Petroleum Geologists; Geologist, Log Analysis Group, Cities Service Oil Company, Summer, 1978; Teaching Assistant, Oklahoma State University, 1978-79; Geologist, West Texas-New Mexico Projects Group, Amoco Production Company, Summer, 1979; Teaching Assistant, Oklahoma State University, 1979-1980; Well-site Geologist, self employed, 1980-1981; Geologist, Earth Energy Resources, Inc., January, 1981 to November, 1981; Geologist, Coquina Oil Corp., November, 1981 to present.